JCI insight

Single-cell immune transcriptomics reveals an inflammatory–inhibitory set-point spectrum in autoimmune diabetes

Ivan I. Golodnikov, Elizaveta S. Podshivalova, Vadim I. Chechekhin, Anatoliy V. Zubritskiy, Alina A. Matrosova, Nikita A. Sergeev, Margarita D. Samsonova, Yaroslav V. Dvoryanchikov, Tatiana V. Nikonova, Ekaterina V. Bondarenko, Marina Yu. Loguinova, Yulia A. Medvedeva, Dmitry N. Laptev, Rita I. Khusainova, Ildar R. Minniakhmetov, Marina V. Shestakova, Natalia G. Mokrysheva, Ivan I. Dedov

JCI Insight. 2025. https://doi.org/10.1172/jci.insight.199050.

Research In-Press Preview **Endocrinology** **Genetics**

Autoimmune diabetes encompasses rapidly progressive type 1 diabetes mellitus (T1D) and indolent latent autoimmune diabetes in adults (LADA), representing distinct inflammatory set points along a shared autoimmune spectrum. Yet the immunological mechanisms that determine these divergent inflammatory states remain unresolved. We performed single-cell RNA sequencing with paired T and B cell receptor profiling on over 400,000 peripheral blood mononuclear cells (PBMCs) from patients with LADA, newly diagnosed T1D, and healthy controls. PBMC composition was comparable across cohorts, indicating that qualitative rather than quantitative immune differences underlie disease heterogeneity. In T1D, pan-lineage activation of NF-κB, EGFR, MAPK, and hypoxia pathways, coupled with a TNF-centered communication hub, enhanced MHC signaling, and disrupted adhesion, promoted systemic inflammation. LADA, by contrast, exhibited global suppression of NF-κB/EGFR activity, retention of moderate JAK/STAT tone, reinforced natural killer cell inhibitory checkpoints via HLA-C–KIR2DL3/3DL1 interaction, and stabilized $CD8^+$ T cell synapses through HLA-C–CD8 binding, collectively restraining effector activation. Single-cell V(D)J analysis revealed multiclonal, patient-unique adaptive repertoires, emphasizing the primacy of signaling context over receptor convergence. These findings define autoimmune diabetes as an inflammatory–inhibitory set-point continuum, positioning the NF-κB/EGFR–JAK/STAT gradient and HLA-C–KIR axis as potential therapeutic targets to preserve residual β-cell function.

Find the latest version:

https://jci.me/199050/pdf

Manuscript title:

Single-cell immune transcriptomics reveals an inflammatory–inhibitory set-point spectrum in autoimmune diabetes

Authors

Ivan I. Golodnikov[1], Elizaveta S. Podshivalova[1], Vadim I. Chechekhin[1,2], Anatolii A. Zubritskiy[1,3], Alina A. Matrosova[1], Nikita A. Sergeev[1], Margarita D. Samsonova[1], Yaroslav V. Dvoryanchikov[1], Tatiana V. Nikonova[1], Ekaterina V. Bondarenko[1], Marina Yu. Loguinova[1], Yulia A. Medvedeva[1,3], Dmitry N. Laptev[1], Rita I. Khusainova[1], Ildar R. Minniakhmetov[1], Marina V. Shestakova[1], Natalia G. Mokrysheva[1], Ivan I. Dedov[1]

Affiliations

1 Endocrinology Research Centre, Moscow, Russia

2 Medical Research and Educational Institute, Lomonosov Moscow State University, Moscow, Russia

3 Federal Research Centre “Fundamentals of Biotechnology” of the Russian Academy of Sciences, Moscow, Russia

Conflict-of-interest statement

The authors have declared that no conflict of interest exists.

Corresponding author

Ivan I. Golodnikov

11 Dm. Ulyanova street, 117036 Moscow, Russian Federation,

Tel:+7 985-352-05-75,

Email: miloru9@gmail.com

Abstract

Autoimmune diabetes encompasses rapidly progressive type 1 diabetes mellitus (T1D) and indolent latent autoimmune diabetes in adults (LADA), representing distinct inflammatory set points along a shared autoimmune spectrum. Yet the immunological mechanisms that determine these divergent inflammatory states remain unresolved. We performed single-cell RNA sequencing with paired T and B cell receptor profiling on over 400,000 peripheral blood mononuclear cells (PBMCs) from patients with LADA, newly diagnosed T1D, and healthy controls. PBMC composition was comparable across cohorts, indicating that qualitative rather than quantitative immune differences underlie disease heterogeneity. In T1D, pan-lineage activation of NF-κB, EGFR, MAPK, and hypoxia pathways, coupled with a TNF-centered communication hub, enhanced MHC signaling, and disrupted adhesion, promoted systemic inflammation. LADA, by contrast, exhibited global suppression of NF-κB/EGFR activity, retention of moderate JAK/STAT tone, reinforced natural killer cell inhibitory checkpoints via HLA-C–KIR2DL3/3DL1 interaction, and stabilized $CD8^+$ T cell synapses through HLA-C–CD8 binding, collectively restraining effector activation. Single-cell V(D)J analysis revealed multiclonal, patient-unique adaptive repertoires, emphasizing the primacy of signaling context over receptor convergence. These findings define autoimmune diabetes as an inflammatory–inhibitory set-point continuum, positioning the NF-κB/EGFR–JAK/STAT gradient and HLA-C–KIR axis as potential therapeutic targets to preserve residual β-cell function.

Introduction

Latent autoimmune diabetes in adults (LADA) is a form of autoimmune diabetes characterized by serological hallmarks typical of type 1 diabetes mellitus (T1D), including β-cell autoantibodies and T-cell–mediated insulitis, but with a notably delayed onset and slower decline in endogenous insulin secretion. Clinically, this indolent progression presents two significant dilemmas: (i) identifying individuals who would benefit from early immunomodulatory intervention, and (ii) preserving residual β-cell function after the onset of autoimmune destruction (1, 2). A central mechanistic uncertainty remains unresolved: does LADA represent merely a milder phenotype on the autoimmune diabetes spectrum, or do specific immunoregulatory mechanisms actively restrain islet cytotoxicity, moderating disease severity (3)? In this study, we adopt the framework of autoimmune diabetes as a clinical and immunological spectrum, while adjusting for age to minimize confounding between LADA and new-onset T1D.

Peripheral immunophenotyping reveals largely overlapping distributions of major leukocytes between individuals with LADA and T1D. Specifically, frequencies of IFN-γ^+ $CD4^+$ and $CD8^+$ T cells, as well as $CD4^+$ effector T cells, appear comparable across both groups. Like T2D patients, LADA patients had increased frequencies of $CD4^+$ Tem and $CD8^+$ Tem cells with respect to T1D (4). A monocyte subpopulation marked by SIGLEC1 and enriched for interferon-response genes was expanded in individuals with LADA and pediatric T1D, suggesting shared features of innate immune activation at disease onset (5). These findings suggest that subtle immunophenotypic differences are insufficient to explain the slower β-cell destruction in LADA; qualitative distinctions in signaling, effector licensing, or checkpoint function are more likely responsible.

Emerging evidence from bulk transcriptomic studies supports this concept of qualitative divergence. Early analyses of LADA patients have revealed heightened expression of pro-inflammatory genes in monocytes (6); RNA sequencing of peripheral neutrophils from newly

diagnosed LADA patients revealed marked enrichment of the nuclear factor κB (NF-κB) signaling pathway, as one of the top-ranked KEGG categories (7); and altered cytokine–cytokine receptor interaction signatures in peripheral-blood mononuclear cells (PBMC) investigated by bulk RNA sequencing (8). However, bulk RNA sequencing inherently averages transcriptional signals across heterogeneous cell mixtures, thereby masking cell-specific transcriptional states and low-frequency pathogenic subsets. Additionally, comparative analyses directly involving newly diagnosed T1D patients alongside LADA cohorts are rare, leaving substantial gaps in understanding precisely which molecular programs differentiate these autoimmune diabetes variants.

We hypothesized that the slower clinical progression of LADA results from selective attenuation of inflammatory signaling cascades, especially NF-κB and growth-factor–related pathways (e.g., EGFR), while simultaneously maintaining sufficient JAK/STAT signaling to sustain chronic, low-grade autoreactivity (9-11). Single-cell RNA sequencing (scRNA-seq), combined with computational pathway inference tools such as PROGENy, permits quantitative characterization of signaling activities at single-cell resolution, revealing functional heterogeneity otherwise obscured by bulk approaches. Such high-dimensional profiling is thus uniquely suited to identifying critical checkpoints that selectively restrain pathogenic effector cells in LADA but fail in rapidly progressing T1D.

Accordingly, we profiled 4.4×10^5 peripheral-blood immune cells from individuals with LADA, newly diagnosed T1D, and matched healthy controls using 5′ single-cell RNA sequencing. We integrated transcriptional data, pathway-activity scores, and cell to cell ligand–receptor interaction analyses to elucidate both cell-intrinsic and intercellular signaling programs underlying differential disease progression. By connecting clinical phenotypes to molecular immune circuitry, this study refines the conceptual framework of autoimmune diabetes pathogenesis and identifies actionable immunological checkpoints, such as the inhibitory HLA-

C/KIR2DL3 axis and regulatory CLEC2D/KLRB1 interactions, as potential therapeutic targets for preserving residual β-cell function in LADA.

Results

Baseline Characteristics of the Study Population

Key demographic and anthropometric characteristics of the study participants are summarized in Supplementary Table S1.

Sex Distribution and Age Differences

Sex distribution was comparable across study groups, with no statistically significant differences detected ($P > 0.05$). Male participants constituted 48% of the T1D cohort, 47% of the LADA cohort, and 50% of the healthy control group. The balanced sex ratio within the control group minimized potential confounding effects in subsequent intergroup comparisons.

In contrast, a statistically significant difference in age was observed between the groups ($P < 0.001$). As anticipated, individuals with T1D exhibited a lower median age of 26 years [21; 31], consistent with the typical onset of autoimmune diabetes in early adulthood. The LADA group showed a significantly higher median age of 40 years [34; 45], reflecting the characteristic later onset of this subtype. The healthy control group had a median age of 33.5 years [27; 42], which was intermediate and broadly comparable to both patient groups, thereby providing an appropriate reference population for age-adjusted analyses.

Body Mass Index and Glycemic Control

Body mass index (BMI) values fell within the normal reference range across all study groups and did not differ significantly ($P = 0.214$), indicating the absence of obesity- or underweight-related confounders in metabolic comparisons.

In contrast, glycated hemoglobin (HbA1c) levels, reflecting long-term glycemic control, varied substantially among groups ($P < 0.001$). The T1D cohort exhibited the highest median HbA1c value 7.8% [6.4; 10.4], consistent with the pronounced hyperglycemia characteristic of early-stage autoimmune diabetes. Participants with LADA demonstrated a moderately elevated median

HbA1c of 7.1% [6.6; 8.8], aligning with prior observations of more gradual β-cell decline in this subtype. As expected, the healthy control group maintained normoglycemic values, with a median HbA1c of 5.1% [4.9; 5.4].

Higher-Resolution Cell Composition Analysis

Compositional analysis reveals no significant differences in cell type proportions among disease groups

We analyzed 442655 single-cell transcriptomes derived from PBMCs of healthy controls (n = 22), patients with LADA (n = 15) and individuals with newly diagnosed T1D (n = 21). Unsupervised clustering and uniform manifold approximation and projection (UMAP) identified ten canonical immune lineages common to all three cohorts (Figure 1A–B, Supplementary Table S2). Relative frequencies of $CD4^+$ and $CD8^+$ T cells, B cells, natural killer (NK) cells, monocytes, dendritic cells, innate lymphoid cells (ILCs), and hematopoietic stem/progenitor cells (HSPCs) did not differ significantly among groups (Figure 1C–D). One-way ANOVA followed by Dunn's post hoc test revealed no statistically significant intergroup differences (all $p > 0.05$).

To further validate the absence of compositional skewing in peripheral immunity, we performed focused high-resolution re-clustering and annotation of all T and NK cells (n = 316,624) across study participants (Supplementary Figure S1A–B, Supplementary Table S3). This analysis resolved 14 transcriptionally distinct immune subsets, corresponding to canonical T- and NK-cell phenotypes. Marker gene and surface protein expression profiles unambiguously delineated naïve, central memory (TCM), effector memory (TEM), cytotoxic (CTL), and tissue-resident memory–like (TRM) $CD4^+$ and $CD8^+$ T-cell subsets, along with $CD56^{bright}$ and $CD56^{dim}$ NK cell populations (Supplementary Figure S1C–D).

Compositional comparisons revealed no statistically significant differences in the frequencies of any T- or NK-cell subset among healthy donors, individuals with LADA, and patients with T1D

(one-way ANOVA, Dunn's post hoc, all $p > 0.05$; Supplementary Figure S1E). Although minor numerical trends were observed, for example, a modest elevation in CD4 TEM cells in LADA none reached significance after multiple-testing correction.

Thus, neither LADA nor T1D shows systemic leukocytosis or lineage-specific PBMC expansion, directing analyses toward qualitative perturbations in gene expression and signaling within a compositionally stable repertoire.

Figure 1

Immune signaling in LADA is attenuated compared to proinflammatory activation in T1D

Differential gene expression analysis was performed using pseudobulk approach in different T and NK cell subtypes. However, the expression changes were minor between study groups, which led us to turn to other methods of qualitative analysis (Figure 2A-D, Supplementary Table S4-6). For further analysis of signaling pathway activity and cell to cell communications we used log2 fold change values of gene expression difference between study groups.

To investigate functional alterations in intracellular signaling, we quantified the activity of 14 canonical signaling cascades: Androgen, epidermal growth factor receptor (EGFR), Estrogen, Hypoxia, Janus kinase–signal transducer and activator of transcription (JAK–STAT), mitogen-activated protein kinase (MAPK), nuclear factor kappa-light-chain-enhancer of activated B cells (NF-κB), tumor suppressor p53, phosphoinositide 3-kinase (PI3K), transforming growth factor beta (TGFB), tumor necrosis factor alpha (TNFA), TNF-related apoptosis-inducing ligand (TRAIL), vascular endothelial growth factor (VEGF), and Wnt signaling across single-cell transcriptomes using the PROGENy algorithm (Figure 2A, E-G; Supplementary Table S7-9). These pathways encompass major immunological domains, including cytokine-driven inflammation (NF-κB, JAK–STAT, MAPK), metabolic and stress response programs (Hypoxia, PI3K, p53), immune regulation (TGFB, TNFA, TRAIL), and trophic or hormonal signaling (EGFR, VEGF, Wnt, Androgen/Estrogen).

Signaling pathway activity in T1D compared to healthy controls

In individuals with newly diagnosed T1D compared to healthy controls, a broad activation of inflammatory signaling was observed across T and NK cells subtypes, with consistent up-regulation of NF-κB, JAK–STAT, and hypoxia-related pathways ($p < 0.05$; Figure 2E, Supplementary Table S8). Subset-specific analysis revealed that naïve and central memory $CD4^+$ and $CD8^+$ T cells additionally exhibited elevated MAPK activity, while cytotoxic and central memory $CD4^+$ T cells demonstrated increased EGFR signaling. Effector memory $CD4^+$ T cells displayed a distinct gain in TGFB activity coupled with a reduction in VEGF pathway engagement.

Among innate lymphocytes, $CD56^{dim}$ NK cells emerged as the only subset showing coordinated up-regulation of PI3K and TGFB alongside the core NF-κB and JAK–STAT module. Down-regulation of signaling was infrequent and largely restricted to isolated reductions in TNFA or VEGF activity, observed in select memory or innate-like subpopulations.

Signaling Pathway Activity in LADA compared to Healthy Controls

In contrast to the pro-inflammatory activation observed in T1D, PBMCs from individuals with LADA exhibited a broadly attenuated signaling profile across immune lineages (Figure 2F, Supplementary Table S7). Among the 14 interrogated pathways, JAK–STAT signaling was the only axis consistently retained across cell types. In contrast, NF-κB, EGFR, TGFB, MAPK, and hypoxia-related pathways were either neutral or suppressed.

In naïve $CD4^+$ and $CD8^+$ T cells, JAK–STAT activation was preserved in the absence of accompanying inflammatory signaling, with concurrent down-regulation of NF-κB and EGFR. Memory T-cell and NK cell subsets exhibited broad suppression of NF-κB and EGFR activity, with occasional modest increases in TNFA or VEGF signaling that did not reach statistical significance after correction.

Notably, regulatory T cells (Tregs) demonstrated the highest JAK–STAT activity within the LADA cohort but this was accompanied by marked suppression of NF-κB, EGFR, and TGFB signaling, suggesting a unique regulatory phenotype distinct from both healthy controls and individuals with T1D.

Signaling Pathway Activity in LADA compared to T1D

T1D is defined by a pancellular NF-κB/JAK-STAT/hypoxia core augmented by subset-specific pro-trophic signals (MAPK, EGFR, PI3K, TGFB). In contrast, LADA retains only focal JAK-STAT or sporadic TNFA/VEGF activity and broadly silences NF-κB-driven inflammation and growth-factor pathways. These quantitative differences provide the molecular framework for the opposing clinical trajectories.

Direct comparison of peripheral immune cells from individuals with LADA and those with newly diagnosed T1D revealed widespread attenuation of signaling pathway activity in LADA (Figure 2G, Supplementary Table S9). Across nearly all immune subsets, nuclear factor NF-κB and EGFR signaling were significantly reduced (adjusted $P < 0.05$). Additional suppression of hypoxia-related and TGFB signaling was observed specifically in effector memory T-cell subsets.

Residual pathway activity in LADA was largely restricted to modest preservation of JAK–STAT signaling, primarily in naïve $CD4^+$ and $CD8^+$ T cells and Tregs. NK cells displayed only a minor up-regulation of TRAIL signaling in $CD56^{bright}$ cells, accompanied by concurrent suppression of NF-κB, EGFR, and Hypoxia pathways. Cytotoxic $CD8^+$ T cells including CTLs, TCM and TEM) subsets, as well as γδ T cells, exhibited pronounced down-regulation of JAK–STAT activity.

Collectively, these findings highlight a striking contrast between disease states: T1D is characterized by a broad, cell-wide activation of NF-κB, JAK–STAT, and hypoxia signaling, further reinforced by subset-specific gains in growth- and survival-related pathways such as MAPK, EGFR, PI3K, and TGFB. In contrast, LADA exhibits focal retention of JAK–STAT

activity and sporadic TNFA or VEGF signaling, while broadly suppressing NF-κB-driven inflammation and trophic signaling. These quantitative differences in immune signaling architecture may underlie the divergent clinical trajectories of rapid β-cell destruction in T1D versus the slower progression observed in LADA.

Figure 2

Immune receptor profiling reveals no disease-specific clonotypes among autoimmune diabetes subtypes

To dissect the specific immunological responses across different subtypes of autoimmune diabetes, we integrated scRNA-seq, T-cell receptor (TCR), and B-cell receptor (BCR) profiling in peripheral blood immune cells from patients with T1D, LADA and healthy controls (Figure 3A). For TCR analysis, only cells that passed scRNA-seq quality control were included, resulting in a subset highlighted in blue (Figure 3A, left). We focused on T cells with available TCR information to investigate clonotype distributions. We found that both healthy donors and patients with different autoimmune diabetes subtypes exhibited entirely distinct expanded T cell clones (Figure 3B-C). These data do not support the presence of specific clonotypes associated with the development of different autoimmune diabetes subtypes. A similar approach was used for BCR analysis (Figure 3A, right), focusing on B cells with available BCR information to examine clonotype distributions. We observed a comparable pattern of clonal expansion among B cells across all donor groups: each donor possessed expanded B cell clones with unique BCRs (Figure 3D-E).

These findings indicate that the T and B cell receptor repertoires in autoimmune diabetes subtypes and healthy donors are entirely private, multiclonal, and non-overlapping, with no evidence of shared or convergent clonotypes across individuals or disease groups.

Figure 3

PD-1 expression is broadly comparable between LADA and T1D

We evaluated PD-1 (*PDCD1*) expression across T cell subsets in LADA, T1D, and healthy controls using log2 fold changes; none of the contrasts reached statistical significance, so all trends should be interpreted cautiously. Focusing on LADA versus T1D, there is no robust differential PD-1 expression in $CD4^+$ or $CD8^+$ lineages: CD4 naive shows a modest negative trend (−0.45), while CD4 TCM (0.33) and CD4 TEM (0.18) trend upward; CD8 TCM is near null (0.09) and CD8 TEM shows a small positive shift (0.31), collectively supporting the view that PD-1 levels are broadly comparable between LADA and T1D in these compartments. Among other T cell populations, the largest non-significant elevation is observed in γδT (log2FC=1.39 in LADA vs T1D), with moderate positive trends in Treg (0.36), MAIT (0.34), and CD4 CTL (0.42); although not statistically supported, the γδT signal could reflect heightened activation or chronic antigenic stimulation and suggests a possible role for γδT-cell regulatory/exhaustion programs in LADA pathogenesis that warrants protein-level and functional validation.

Quantitative mapping of cell–cell signaling reveals amplification of pathogenic immune circuits in T1D and immune balance in LADA

To elucidate how peripheral immune cells coordinate pathogenic signaling in autoimmune diabetes mellitus, we investigated intercellular communication patterns among T-cell and innate-like lymphocyte populations. Aberrant cell to cell interactions are critical mediators of autoimmune tissue damage, facilitating chronic inflammation, recruitment of cytotoxic effectors, and disruption of immunoregulatory feedback loops. In the context of LADA and T1D, dysregulated ligand–receptor signaling may drive the transition from physiological immune surveillance to sustained β-cell–directed autoimmunity. Single-cell resolution mapping of these

communication networks enables identification of functionally distinct axes: pro-inflammatory, adhesive, or inhibitory.

Ligand–receptor inference was performed across the same peripheral immune subsets previously used for intracellular pathway analysis, encompassing the full spectrum of $CD4^+$ and $CD8^+$ T-cell states, regulatory populations and innate-like effectors. Interaction counts between T- and NK-cell subtypes were comparable across donor groups (Figure 3A, Supplementary Figure 2), indicating that disease-specific rewiring reflects the quality rather than the quantity of contacts. Accordingly, subsequent analyses concentrated on quantitative differences in interaction strength and on the specific ligand–receptor pairs that distinguish LADA from T1D.

Peripheral immune landscape in T1D is shaped by discrete, yet inter-locking, ligand–receptor circuits that jointly reinforce β-cell–directed autoimmunity. Seven functional modules dominate this network: (i) a TNF-centered inflammatory and co-stimulatory axis; (ii) enhanced antigen-processing and MHC-II trafficking; (iii) cytoskeletal phosphatase–mediated fine-tuning of T-cell receptor signaling; (iv) global attenuation of adhesion and tissue-homing checkpoints; (v) metabolic reprogramming through basigin–SLC16A7-dependent lactate export; (vi) erosion of NK-cell inhibitory checkpoints driven by diminished β2-microglobulin delivery; and (vii) down-modulation of non-canonical CD40L interactions. The description below details the directionality of each interaction (gain or loss of signal), the predominant cellular sources and recipients, and the inferred mechanistic consequences for T-cell, NK-cell, and myeloid function in the diabetic milieu. By contrast, LADA lacks these circuit amplifications: reinforcement of HLA-C–KIR and LAG3 checkpoints, together with preserved adhesion and metabolic axes, sustains a calibrated low-grade inflammatory state that underpins the immune balance described above.

Cell to cell Communication: T1D versus Healthy Controls

In T1D, the peripheral immune landscape is shaped by a set of discrete yet interdependent ligand–receptor signaling modules that collectively reinforce chronic β-cell–directed autoimmunity. Comparative analysis with healthy controls revealed seven dominant functional clusters that define this aberrant intercellular network, described above.

These modules highlight converging mechanisms of effector amplification, antigenic persistence, and regulatory failure in the peripheral immune milieu of T1D. A comprehensive summary of differentially regulated ligand–receptor interactions, including directionality (gain or loss of signal), predominant source and target subsets, and putative functional consequences is provided in Table 1.

Table 1

Collectively, the seven modules depict a rewired PBMC network that amplifies TNF-driven inflammation, broadens the autoantigenic repertoire, lowers T-cell activation thresholds and weakens metabolic and inhibitory control; these hubs nominate TNFRSF1B, SORL1/CD74 trafficking and KLRC1/CD94 as tractable targets to restore immune balance.

Metabolic inflexibility, marked by suppressed basigin–SLC16A7–mediated lactate export, and erosion of NK cell checkpoint control via diminished β2-microglobulin (B2M)–KLRC1/KLRD1 signaling further compound the loss of immunoregulatory restraint. Downregulation of non-canonical CD40 ligand interactions implies additional defects in antigen-presenting cell (APC)–T cell cross-activation.

By mapping these discrete but converging interaction hubs, our analysis identifies mechanistically distinct and potentially actionable nodes, such as TNFRSF1B signaling, SORL1/CD74 antigen trafficking, and KLRC1/CD94 checkpoint circuits, that may serve as

immunomodulatory targets for preserving immune tolerance and attenuating β-cell autoimmunity in T1D.

Cell to Cell Communication: LADA versus Healthy Controls

LADA exhibits a characteristically slow disease progression, which is paralleled by nuanced yet mechanistically coherent alterations in peripheral immune cell communication. Single-cell–resolved ligand–receptor inference revealed five functionally distinct signaling modules that differentiate individuals with LADA from healthy controls:

1. Reinforcement of MHC class I–KIR inhibitory checkpoints, primarily involving HLA-C and HLA-F ligands engaging KIR2DL3 and KIR3DL1 receptors on $CD56^{dim}$ NK cells, a process consistent with NK-cell "education" and elevated activation thresholds;

2. Stabilization of MHC class I–CD8 co-receptor interactions, through increased engagement of classical (HLA-C) and non-classical (HLA-F) ligands with CD8A/CD8B, may reinforce the TCR–peptide–MHC interface. This may lower the activation threshold of autoreactive cytotoxic T cells and promote a persistent but non-fulminant effector state aligned with the indolent course of LADA.

3. Up-regulation of MHC class II–LAG3 signaling, introducing a negative feedback axis that modulates $CD4^{+}$ T-cell activity through coordinated antigen presentation and inhibitory co-receptor engagement;

4. Augmented CLEC2D–KLRB1 (LLT1–CD161) interactions, supporting the maintenance of tissue-resident mucosal-associated invariant T (MAIT) and γδ T-cell subsets, which may contribute to tissue surveillance and immune modulation;

5. Down-modulation of CD55–ADGRE5 and vimentin–CD44 axes, suggesting dampened complement regulatory signaling and reduced cell–matrix adhesion, potentially limiting

aggressive infiltration and facilitating low-grade inflammation.

Together, these intercellular circuits define a unique immune equilibrium in LADA - one that permits the persistence of autoreactive lymphocytes while simultaneously imposing regulatory constraints that curb fulminant β-cell destruction. This communication profile aligns with the indolent clinical trajectory of LADA and underscores the potential of targeting stabilizing checkpoints rather than broadly suppressing immunity as a strategy to preserve β-cell function (Table 2)

Table 2

Taken collectively, the LADA cell to cell interactome depicts a finely calibrated equilibrium in which inhibitory KIR and LAG3 pathways counterbalance reinforced MHC-I and MHC-II antigen presentation, while innate-like CLEC2D–KLRB1 signaling and attenuated adhesion/complement checkpoints sustain low-grade inflammation. This composite wiring raises activation thresholds for uncontrolled β-cell destruction yet maintains sufficient effector tone to drive slow β-cell attrition over time. By pinpointing nodal interactions, particularly KIR2DL3/HLA-C, CD8AB/HLA-C, and CLEC2D/KLRB1, the present analysis delineates therapeutic entry points for selective immune recalibration aimed at preserving residual β-cell function in LADA.

Cell to Cell Communication: LADA versus T1D

Direct single-cell ligand–receptor mapping contrasting LADA with T1D reveals six mechanistic modules that collectively decelerate, but do not extinguish β-cell directed autoimmunity in LADA. These intercellular circuits configure a tightly calibrated immune network that stands in stark contrast to the broadly pro-inflammatory and cytolytic architecture characteristic of T1D.

1. Augmented MHC class I–KIR inhibitory signaling, primarily via HLA-C ligation of KIR2DL3 and, to a lesser extent, KIR3DL1, elevates the activation threshold of $CD56^{bright}$ natural killer (NK) cells. This enhancement of NK-cell "education" may suppress nonspecific β-cell cytotoxicity and preserve immune restraint.

2. Reinforcement of MHC class I–CD8 co-receptor binding, through up-regulated HLA-C and CD8A/B interactions, is hypothesized to enhance co-receptor recruitment of LCK (lymphocyte-specific protein tyrosine kinase), thereby stabilizing TCR–peptide–MHC complexes. This may sustain cytotoxic T-cell activity at a sub-lytic threshold compatible with slow β-cell attrition.

3. Lymphotoxin-β (LTB)–TNFR1 signaling, selectively up-regulated in $CD56^{bright}$ NK cells, may fine-tune cytokine release profiles, such as IFN-γ and TNF superfamily members, without triggering the full pro-inflammatory cascade observed in T1D.

4. Enhanced LLT1–CD161 (CLEC2D–KLRB1) interactions, prominently involving MAIT and γδ T-cell subsets, support the maintenance of tissue-resident effector populations that propagate controlled, IL-17/IFN-γ–mediated inflammatory responses without precipitating aggressive cytolysis.

5. Neuro-immune modulation via adrenergic and ion-channel signaling, including up-regulation of ARPC5–ADRB2 and CALM3–KCNQ5 ligand–receptor axes, suggests sympathetic nervous system input into effector-cell calibration. While mechanistically plausible, these interactions remain putative and require functional validation.

6. Partial erosion of the complement–adhesion checkpoint, marked by downregulation of CD55–ADGRE5 signaling, may limit deep tissue infiltration of lymphocytes but simultaneously delay the resolution of inflammation, contributing to the low-grade, smoldering immune tone characteristic of LADA.

Together, these intercellular mechanisms shape a peripheral immune architecture in LADA that allows for persistent, autoreactive immune activity while preventing the abrupt β-cell destruction typical of T1D. This equilibrium may offer a therapeutic window for selective immune recalibration that preserves β-cell function without impairing global immune competence (Table 3).

Table 3

The LADA interactome thus represents a finely balanced equilibrium in which strengthened NK-cell checkpoints counter-poise a modestly lowered CD8 activation threshold; regulatory TNF-superfamily and neuro-immune cues dampen overt Th1 polarization; and attenuated complement–adhesion safeguards sustain low-grade, chronic inflammation. This wiring pattern slows β-cell attrition while preserving sufficient effector tone to drive gradual dysfunction, mechanistically explaining LADA's protracted clinical course. Therapeutically, well-supported interaction nodes, HLA-C/KIR2DL3, the LCK-linked CD8A/B complex, CLEC2D/KLRB1 and CD55/CD97 stand out as plausible targets for precision immunomodulation. In contrast, other pairs such as HLA-C–KIR3DL1, ARPC5–ADRB2 and CALM3–KCNQ5 remain preliminary and should undergo focused biochemical validation before being considered for clinical development.

Multiplex serum cytokine analysis

Orthogonal serum profiling corroborated the single-cell inferences. Compared with LADA, patients with new-onset T1D exhibited higher concentrations of sCD40L (16 823 [14067; 19766] vs 9754 [6460; 13179] pg/mL), IL-12p70 (53.4 [41.1–159.9] vs 27.5 [7.9; 56.3] pg/mL), RANTES (3336 [2561–3589] vs 2467 [2224–2961] pg/mL), FGF2 (523 [305–868] vs 256 [152–610] pg/mL), and IL-1α (3.82 [2.73–5.84] vs 2.5 [1.63–2.87] pg/mL; all $P < 0.05$ within the prespecified subset). These elevations are consistent with an enhanced CD40 costimulatory axis, heightened Th1 polarization, pro-inflammatory chemokine signaling, and growth-factor–linked

tissue remodeling in T1D, collectively reinforcing the functional relevance of the signaling gradients identified at single-cell resolution.

DISCUSSION

Cell composition

Single-cell profiling revealed no significant differences in peripheral proportions of $CD4^+$ and $CD8^+$ T, B, NK, monocytes, or dendritic cells among LADA, new-onset T1D and controls, indicating a conserved bulk immune landscape. This contrasts with earlier flow-cytometric reports of higher effector-memory $CD8^+$ T-cells, altered B-cell subsets and increased activated NK-cells in LADA versus T1D (4, 12, 13). Our scRNA-seq data therefore suggest that such shifts, if present, are modest and do not yield overt compositional skewing.

The key factor is individual heterogeneity: each patient shows a unique transcriptomic profile. Even after matched cohort selection and batch correction, diagnosis explained minimal variance, with no significant compositional shifts (14).

Immune Pathways Driving β-Cell Destruction

Single-cell profiling exposes a clear signaling dichotomy between LADA and new-onset T1D. In LADA, NF-κB- and EGFR-associated activities are broadly dampened, whereas T1D displays their full activation; JAK-STAT signaling is elevated in both diseases but peaks in T1D. These patterns indicate fundamentally different inflammatory set points: T1D operates in a high rate, proliferative milieu, whereas LADA maintains a muted, “dialed-down” immune tone.

NF-κB

NF-κB drives pro-inflammatory gene expression and β-cell apoptosis in T1D (15, 16). Our data show robust NF-κB activation in T1D but attenuated in LADA, likely limiting cytokine storms and antigen-presenting cell (APC) activation (17).

EGFR

EGFR signaling, linked to cell growth and tissue repair, is likewise heightened in T1D yet minimal in LADA. In β-cells, EGFR is required for compensatory proliferation after injury (18, 19); its up-regulation in T1D may reflect both vigorous immune-cell expansion and an unsuccessful regenerative response. Regulatory T cells can supply the EGFR ligand amphiregulin during murine insulitis (20), suggesting that the pronounced EGFR signature in T1D mirrors an acutely remodeling islet niche. The near-baseline EGFR activity in LADA implies less tissue damage and a correspondingly restrained repair program.

JAK–STAT

The JAK–STAT axis integrates multiple cytokine cues, notably IFN-γ, to heighten MHC-I expression on β-cells and intensify autoimmune targeting (21). Clinical and pre-clinical studies demonstrate that JAK1/2 inhibition (e.g., baricitinib, AZD1480) can preserve endogenous insulin production (22, 23). In our dataset, JAK-STAT activity forms a monotonic gradient, highest in T1D, intermediate in LADA, lowest in controls, underscoring its quantitative contribution to β-cell loss and validating it as a tractable biomarker and therapeutic target.

Together, these contrasts position LADA and T1D along an inflammatory continuum, with NF-κB/EGFR suppression and moderated JAK-STAT activity in LADA versus full pathway activation in T1D.

T- and B-Cell Receptor Repertoires

Single-cell V(D)J profiling confirmed highly private, multiclonal TCR and BCR landscapes across LADA, recent-onset T1D, and controls: no shared CDR3 sequences or over-represented V/J combinations emerged, corroborating earlier findings that islet-reactive lymphocytes seldom form public clonotypes in blood. This heterogeneity stems from two factors. (1) HLA diversity imposes idiosyncratic thymic selection, yielding patient-specific solutions to β-cell epitopes. (2) Tissue sequestration concentrates pathogenic clones in islets and draining nodes; deep

sequencing shows oligoclonal expansions there are absent or singletons in blood, representing <1 % of the peripheral repertoire. The same applies to B cells: the lone "public" IgH clone reported earlier is neither disease-specific nor reproducible. Hence, disease tempo depends less on convergent receptor usage than on qualitative cues, cytokine milieu, checkpoint balance, metabolic state, that tune activation of these private clones. Targeting shared signaling nodes (e.g., JAK-STAT, HLA-C–KIR) may therefore be more broadly effective than clonotype-specific approaches (24-28).

Ligand–receptor analysis

Single-cell ligand–receptor mapping shows a fundamental rewiring of intercellular crosstalk along the diabetes spectrum. New-onset T1D displays an expansive, TNF-centric hub connecting T and innate cells, highlighted by TNF–TNFRSF1B and TNF–TRADD pairs, far exceeding healthy levels. This surge, together with TNF-driven co-stimulatory links such as TNF–ICOS, lowers T-cell activation thresholds and amplifies bystander recruitment, cohering with TNF's dominant β-cell cytotoxicity in acute disease (1, 29). LADA PBMCs, by contrast, lack a comparable TNF module; macrophage-derived IL-1β predominates, curbing direct β-cell damage and moderating overall inflammation. Hence, T1D is wired for maximal pro-inflammatory signaling, whereas LADA retains a selectively attenuated, calibrated interactome.

Beyond cytokines, antigen-presentation circuits diverge sharply. T1D exhibits heightened antigen-processing and MHC-II trafficking (e.g., LRPAP1–SORL1, COPA–CD74) (30, 31), expanding autoantigen loading, fostering epitope spreading, and sustaining broad T-cell priming, hallmarks of rapid-onset disease with multiple autoantibodies. LADA shows no such up-regulation, implying a narrower antigenic drive consistent with its tempered cytokine milieu.

Conversely, LADA displays enhanced HLA-C–CD8A/B engagement, stabilizing TCR–pMHC interactions and recruiting LCK, thereby allowing $CD8^+$ CTLs to operate at a low, persistent "simmer" (32). These synapses likely support restrained effector activity that aligns with the

slower β-cell attrition and the reduced proliferative vigor of LADA autoreactive T cells (1). Thus, T1D favors maximal antigenic stimulation, whereas LADA pairs focused antigen engagement with regulatory restraint.

A defining hallmark of LADA is its reinforced inhibitory circuitry. Single-cell mapping shows greater engagement of HLA-C and HLA-F ligands with inhibitory KIR2DL3 and KIR3DL1 on NK cells, contrasting sharply with the attenuated contacts in T1D. These stronger KIR–HLA-C interactions likely reflect the superior inhibitory capacity of specific KIR/HLA allelic pairs; studies demonstrate that even closely related receptors (e.g., KIR2DL2 vs. KIR2DL3) dock HLA-C with distinct geometries and avidities, driving functional heterogeneity (33). In T1D the checkpoint erodes: reduced β2-microglobulin loading diminishes MHC-I display, triggering "missing-self" recognition and unleashing NK cytotoxicity (34). LADA's up-regulated KIR signaling instead preserves an "educated-self" state, curbing unwarranted β-cell lysis, consistent with genetic data linking certain KIR/HLA combinations to T1D protection, an axis still under-explored in LADA (35, 36).

Parallel restraint operates in the T-cell compartment. LADA shows heightened MHC-II engagement of the inhibitory receptor LAG-3 on $CD4^+$ T cells, forming a feedback loop that limits proliferation (37); this axis remains largely silent in T1D. Collectively, enhanced KIR and LAG-3 signaling allows autoreactive lymphocytes to persist in LADA but under tighter surveillance, helping explain its slower, less destructive course compared with T1D.

Additional divergence occurs in adhesion and metabolic signaling. T1D PBMCs display broad suppression of homing interactions, diminished ITGAL/ITGAM–ICAM2 binding and weaker IL-16–KCNA3 chemoattractant signaling, suggesting impaired integrin-mediated transmigration and tissue residency (38, 39). Chronic hyper-activation may drive receptor shedding/internalization, leaving highly inflammatory cells sequestered in blood or lymphoid

tissue and relying on TNF-mediated endothelial disruption rather than orderly diapedesis to reach islets (40). LADA retains these adhesion axes, supporting regulated, low-grade infiltration.

Metabolically, T1D lymphocytes down-regulate the basigin–SLC16A7 lactate-export pathway, limiting glycolytic efflux. Resultant acid accumulation echoes tumor-associated T-cell exhaustion and can dampen effector function despite heightened activation (41, 42). LADA lacks this defect: its immune cells operate below the metabolic redline, sustaining activity without overt burnout. Thus, T1D couples aggressive cytokine output with compromised migration and metabolic stress, whereas LADA maintains balanced trafficking and bioenergetic resilience.

Our interactome also revealed auxiliary signaling axes that diverge between diseases. T1D down-modulates CD40L–ITGAM and CD40L–CD53 contacts non-canonical T-cell/APC links independent of the classic CD40 pathway (43). Their loss suggests T-cell co-stimulation is funneled into a single, highly pro-inflammatory CD40 route, or represents a compensatory brake against further activation. LADA retains these interactions, supporting more nuanced, balanced synapses.

Conversely, LADA uniquely up-regulates CLEC2D–KLRB1 signaling on MAIT/γδ subsets, sustaining tissue-resident IL-17/IFN-γ production without triggering acute β-cell cytolysis, whereas T1D skews toward overt Th1 cytotoxicity (44, 45). LADA also shows selective neuro-immune crosstalk ARPC5–ADRB2 and CALM3–KCNQ5 implicating adrenergic and ion-channel inputs in fine-tuning immunity (46, 47). Collectively, these modulatory circuits add incremental restraints that help keep LADA's autoimmune response below the destructive threshold characteristic of T1D.

Our findings were further supported by multiplex serum profiling, which revealed higher concentrations of sCD40L, IL-12p70, RANTES, FGF2, and IL-1α in T1D relative to LADA. These systemic readouts independently align with the TNF/CD40 costimulatory hub, Th1/JAK–STAT skewing, NF-κB–linked cytokine induction, and growth-factor pathways inferred from our

single-cell data. While circulating cytokine levels cannot fully capture islet-resident immune dynamics, their concordance with transcriptomic signatures reinforces the biological validity of the observed signaling divergence.

In summary, cell to cell communication networks in LADA vs. T1D underscore a fundamental difference in immune balance. T1D is driven by potent amplification loops – TNF-centric inflammation, maximal antigen presentation, lowered activation thresholds, and lifted inhibitory checkpoints – creating a perfect storm for rapid β-cell annihilation. LADA, on the other hand, embodies a state of immune equipoise: autoreactive cells are present and even primed, but they operate under heightened inhibitory surveillance, metabolic and migratory constraints, and alternative signaling that collectively enforce restraint. This delicate equilibrium in LADA's immune crosstalk permits slow burn autoimmunity, often allowing patients to retain β-cell function for years. From a therapeutic standpoint, mapping these divergent communication hubs points to tangible targets for intervention. In T1D, disrupting the TNF–TNFR axis or enhancing metabolic fitness of T cells might dampen the wildfire inflammation. In LADA, bolstering inhibitory pathways like KIR/HLA-C or LAG3, or reinforcing adhesion checkpoints, could further tip the scales toward protection without extinguishing the necessary immune surveillance. Notably, some ligand–receptor pairs identified here (for example, HLA-C–KIR2DL3 or CD8–HLA strengthening via LCK) coincide with known regulatory nodes in autoimmunity and are ripe for mechanistic exploration. By leveraging such insights, we can aim to recalibrate the immune network – quieting the excessive crosstalk in T1D and fortifying the self-restraint in LADA – to preserve pancreatic β-cells while maintaining overall immune competence.

The pathogenesis of autoimmune diabetes unfolds across multiple biological levels, as demonstrated in previous studies. In the peripheral blood mononuclear compartment (PBMC), a pro-inflammatory immune bias is already apparent. $CD4^+$ T-helper 1 cells (T-bet↑) secrete IFN-γ and IL-2, licensing the expansion and cytotoxic maturation of $CD8^+$ T cells and NK cells, whereas Th17 cells (RORγt↑) produce IL-17A, fostering monocyte recruitment (48, 49).

Concomitantly, quantitative and functional attrition of $FOXP3^+$ T-regulatory cells weakens peripheral tolerance (50, 51). B-cell dysregulation manifests as autoreactive clones synthesising insulin, GAD65, IA-2 and ZnT8 antibodies, while the innate compartment, classical monocytes exhibit NF-κB and STAT1/3 activation, further amplifying systemic priming (52, 53).

Antigen-laden dendritic cells traffic via the lymphatics to pancreatic-draining lymph nodes, where β-cell peptides are displayed on MHC I/II, driving clonal expansion of $CD8^+$ cytotoxic and $CD4^+$ effector subsets together with germinal-centre maturation of B cells (54). The emerging repertoires are oligoclonal and individualised, lacking a universal public TCR, yet collectively they seed the circulation and home to the pancreas along (55).

Within the islets of Langerhans, infiltrating $CD8^+$ CTLs and NKG2D NK cells execute granzyme-B/perforin-mediated β-cell lysis, while Th1- and Th17-derived cytokines (IFN-γ, IL-17A) heighten local inflammation and numerically insufficient Tregs fail to restore restraint (56, 57). Stressed β-cells characterised by HLA-I up-regulation, ER perturbation and CXCL10 release activate JAK-STAT1/3, NF-κB, PI3K–AKT–mTOR and MAPK p38/JNK pathways, culminating in apoptosis, secondary antigen liberation and epitope spreading (58-60). Type I interferons perpetuate this feed-forward loop, establishing chronic pancreatic inflammation that feeds back into systemic immune activation and metabolic dysregulation.

As with most human diabetes studies, our analyses were confined to peripheral blood rather than islet tissue, limiting direct mechanistic inference. To synthesize the above observations, we present an updated, multi-tier model of autoimmune diabetes pathogenesis (Figure 4) that incorporates the key single-cell discoveries of this study. Specifically, the diagram highlights (i) the selective dampening of NF-κB- and EGFR-driven signaling cascades in LADA, contrasted with their robust activation in new-onset T1D, while JAK-STAT activity remains comparably elevated in both conditions; (ii) the strengthened inhibitory checkpoint formed by HLA-C engagement of KIR2DL3/3DL1, which raises the activation threshold of NK cells in LADA; (iii)

reinforcement of the HLA-C–CD8A/B co-receptor complex that stabilizes low-affinity cytotoxic T-cell interactions without precipitating fulminant β-cell lysis; (iv) augmented CLEC2D–KLRB1 signaling that sustains a tissue-resident, low-grade inflammatory tone; and (v) the absence of major shifts in peripheral immune-cell composition, underscoring that qualitative, rather than quantitative, rewiring of immune circuitry distinguishes LADA from T1D. Together these integrated elements provide a coherent framework explaining how LADA maintains chronic, yet restrained, β-cell autoimmunity, whereas T1D is driven by an unchecked pro-inflammatory network that accelerates β-cell destruction. Our data do not establish LADA as a distinct disease entity. Rather, they support the interpretation of LADA and T1D as points along an autoimmune diabetes continuum, differentiated by inflammatory set-points and rate of β-cell decline. Although age was modeled as a covariate, residual influences of age and disease duration cannot be fully excluded.

Figure 4

Limitations and Future Directions

Our study has several limitations that should be acknowledged. First, it is cross-sectional and thus cannot establish temporal causality. Second, although age was modeled as a covariate, residual influences of age and disease duration cannot be fully excluded. Median HbA1c values were comparable between T1D and LADA (7.8% vs. 7.1%), and all T1D patients as well as 11 of 15 LADA patients were on insulin therapy, minimizing—but not eliminating—the contribution of metabolic control and treatment status. Third, our analyses relied on PBMC rather than islet-infiltrating cells, which may differ in situ. Fourth, we did not perform orthogonal functional assays such as immunoblotting or receptor blockade to directly test HLA-C–KIR or HLA-C–CD8 interactions. Finally, the absence of an independent replication cohort limits the generalizability of our findings. These caveats underscore the need for future longitudinal and mechanistic studies to validate and extend our observations. Nevertheless, by integrating single-

cell transcriptomics with multiplex cytokine profiling, our work provides a framework that generates testable hypotheses for follow-up functional and clinical investigations.

Materials and Methods

Sex as a biological variable

Both male and female participants were enrolled. Sex was not used as a stratification factor, and no sex-specific analyses were performed. Findings are expected to be relevant to both sexes.

Study design and participants

Participants were not randomized, and group allocation was known to investigators prior to analysis, as clinical group designation was essential for stratification and subsequent comparative analyses.

This was a single-center, cross-sectional, observational study. Participants were recruited consecutively, including all eligible individuals who received either inpatient or outpatient care at the study site during the enrollment period.

This study was conducted at the Endocrinology Research Center, Ministry of Health of the Russian Federation, between February 2023 and December 2024. A total of 58 individuals were enrolled and stratified into three groups: healthy controls (n = 22), patients with newly diagnosed type 1 diabetes mellitus (T1D; disease duration ≤1 year, n = 21), and patients with latent autoimmune diabetes in adults (LADA; disease duration ≤5 years, n = 15). Detailed inclusion and exclusion criteria are summarized in Table 4.

Table 4

Clinical Assessments

Fasting plasma glucose and glycated hemoglobin (HbA1c) levels were measured using the Architect c8000 automated biochemical analyzer (Abbott Laboratories, USA), following protocols standardized by the National Glycohemoglobin Standardization Program (NGSP).

Sample Collection and Processing

The work was carried out using the materials of the Unique Scientific Facility “Collection of Biological Material from Patients with Endocrine Pathologies” of the Endocrinology Research Center (Moscow, Russia).

Venous blood collected for fasting glucose and HbA1c into BD Vacutainer® tubes with gel separator or EDTA (4 mL). PBMCs were isolated from whole blood in BD Vacutainer® CPT tubes with sodium heparin and ficoll (8 mL) and processed within 2 hours at room temperature.

PBMCs were isolated by centrifugation in a horizontal rotor (swing-out head) at 20°C for 20 minutes at 1,800 RCF. The upper 5 mL of plasma was discarded, and the remaining fraction, including the PBMC layer, was transferred to 50 mL conical tubes for washing. Cells were washed twice with 1× phosphate-buffered saline (PBS) supplemented with 1% heat-inactivated fetal bovine serum (FBS; HyClone, USA) and 1 mM EDTA, followed by centrifugation at 300 RCF for 10 minutes. Residual red blood cells were lysed using ACK Lysing Buffer (Thermo Fisher Scientific, USA), followed by additional wash and centrifugation steps. The final PBMC pellet was resuspended in CryoStor® CS10 (StemCell Technologies, Canada) and stored at −80°C (short-term) or −150°C (long-term).

Sample Preparation for Single-Cell RNA Sequencing

Cryopreserved PBMCs were rapidly thawed in a 37°C water bath for 3 minutes, then transferred gently into 14 mL of RPMI-1640 medium (PanEco, Russia) supplemented with 10% heat-inactivated fetal bovine serum (FBS; HyClone, USA). Cells were centrifuged at 20°C for 10 minutes at 300 RCF, and the resulting pellet was resuspended and passed through a 30-µm MACS SmartStrainer (Miltenyi Biotec, Germany) to remove cell aggregates. All subsequent procedures were performed on ice to preserve cell viability and transcriptome quality.

Viable cell numbers were determined using trypan blue exclusion with the Countess 3 FL automated cell counter (Thermo Fisher Scientific, USA). The final cell suspension was adjusted

to a concentration of 3,000 cells/μL in RPMI-1640 supplemented with 10% FBS for downstream single-cell library preparation.

Single-cell RNA Sequencing

Single-cell RNA sequencing (scRNA-seq) was performed using the Chromium Next GEM Single Cell 5′ Reagent Kits v2 (Dual Index) according to the manufacturer's protocol (10x Genomics, USA). PBMC suspensions containing approximately 50,000 cells per sample were loaded into microfluidic chips and processed using the Chromium Controller for single-cell partitioning and barcoding.

Library quality was assessed using the Qubit™ dsDNA High Sensitivity Assay Kit (Thermo Fisher Scientific, USA) for DNA quantification and the Agilent High Sensitivity D1000 ScreenTape Assay (Agilent Technologies, USA) for fragment size analysis. Sequencing was performed on the NovaSeq 6000 platform (Illumina, USA) using the NovaSeq 6000 S4 Reagent Kit v1.5 (300 cycles) in paired-end mode (151–10–10–151), with libraries multiplexed at concentrations of 1.3-1.4 nM for 5' gene expression libraries (standard NovaSeq protocol) and 1-1.1 nM for V(D)J libraries (NovaSeq XP protocol). The expected sequencing depth was approximately 80,000 read pairs per cell for 5' gene expression library and about 15,000 read pairs for V(D)J library

Single-cell RNA-seq analysis

Raw sequencing scRNA-seq data were processed using bcl2fastq2 12.20 to generate FASTQ files. Reads were aligned to the GRCh38-2020-A human reference genome using Cell Ranger 7.1.0. Ambient RNA contamination was removed using SoupX 1.6.2, and doublets were identified using scDblFinder 1.12.0 in R 4.2.1. High-quality cells were retained based on the following criteria: mitochondrial gene content <6%, heat shock protein gene content <2%, and at least 200 expressed genes per cell.

Further analyses were conducted using scanpy 1.10.2 in Python 3.9.16. Data were log-normalized, and 2000 variable genes were identified with the seurat_v3 method. Integration was performed using scANVI. Cell type annotation was performed with scParadise and Azimuth, supplemented by marker databases (CellMarker 2.0, PanglaoDB, GeneCards). Surface protein data imputation was performed using pretrained Human_PBMC_3p scEve model from scParadise tool. Differential gene expression analysis between cell populations was conducted in scanpy 1.10.2 using wilcoxon test. We used the following criteria to filter differentially expressed genes for generating cell type-specific marker gene lists: log2foldchange > 1.0, proportion of cells within the cell type where the gene is detected > 0.2, and Benjamini-Hochberg adjusted p-value < 0.05. Differential gene expression analysis between donors was performed using pseudobulk analysis with pyDeSeq v0.4.12. Statistical analysis of differential gene expression was conducted using the Wald test with Benjamini-Hochberg p-value correction. Age was included as a covariate in all differential expression and pathway models to reduce potential confounding between LADA and T1D cohorts.

Signaling pathway activity was determined using a multivariate linear model in decoupler 1.8.0 and the PROGENy database. Signaling pathway activity inference was performed using the log2fold change values from the list of differentially expressed genes. Statistical testing of signaling pathway activity was performed using Student's t-test with Benjamini-Hochberg p-value correction. Cell composition analysis across the study groups was conducted using pertpy 0.9.4

Ligand-receptor interaction analysis was performed using liana (v1.5.0). To enhance robustness and reduce methodological bias, we used an aggregate score that integrates results from five independent methods: CellPhoneDB, Connectome, log2FC, NATMI, and SingleCellSignalR. A consensus database of ligand-receptor interactions was also used to maximize the scope of detected interactions. We used differentially expressed genes previously identified for different donor groups to reflect variations in ligand and receptor expression between diabetes subtypes.

This strategy enabled the identification of communication events specific to particular groups and provided additional biological insight.

Single-cell TCR/BCR-seq analysis

Raw sequencing scTCR/BCR-seq data were processed using bcl2fastq2 12.20 to generate FASTQ files. Cell Ranger 7.1.0 and bcl2fastq2 12.20 to generate FASTQ files. Reads were aligned to the vdj-GRCh38-alts-ensembl-7.1.0 human reference genome using Cell Ranger 7.1.0. We performed quality control of TCR and BCR data by retaining only those cells that passed the quality control filtering during the processing of the scRNA-seq gene expression matrices. Thus, only cells with high-quality transcriptomic profiles were included in the subsequent TCR/BCR analyses. Cells were grouped into clonotypes based on the nucleotide sequence identity (for TCR data) and 80% similarity (for BCR data) of the CDR3 region. We used at least 50 cells (for TCR data) and 3 cells (for BCR data) for clonotype network visualization (61-78).

Multiplex serum cytokine analysis

- The level of various immunoregulatory factors in the serum was measured using a commercial kit (MILLIPLEX Human Cytokine/Chemokine/Growth Factor Panel A 48 Plex Premixed Magnetic Bead Panel, HCYTA-60K-PX48, Millipore Sigma, United States) using the MAGPIX (Luminex Corp, United States). The analysis was performed according to the manufacturer's instructions. xPONENT 4.1 Software was used to obtain the raw data. The concentrations of 48 cytokines were determined using standard curves.

Statistical analysis of clinical data

Clinical and cytokine data were analyzed in Statistica (v13). Continuous variables are presented as median [IQR] and were compared using the Kruskal–Wallis test followed by two-tailed

Mann–Whitney U post hoc comparisons. Categorical variables were analyzed using the χ^2 test. A P value less than 0.05 was considered statistically significant.

Use of artificial intelligence

Generative AI (GPT-4o) was used to assist with English-language editing and partial translation of the manuscript from Russian. All scientific content was written, reviewed, and verified by the authors.

Study approval

The study was approved by the Local Ethics Committee of the Endocrinology Research Centre (Protocol No. 18, October 12, 2022). Written informed consent was obtained from all participants.

Data availability

ScRNA-seq data generated for this manuscript is available in GEO database under the accession number: GSE308968. Supporting data values underlying all main and supplementary figures are provided in the accompanying Excel file ‘Supporting_Data_Values.xlsx’.

CONCLUSION

In this single-cell study we constructed a high-resolution immune atlas of latent autoimmune diabetes in adults and new-onset type 1 diabetes, analysing more than 4×10^5 peripheral-blood mononuclear cells together with paired V(D)J repertoires. Contrary to earlier flow-cytometric reports we found no quantitative shift in the frequencies of major lymphoid or myeloid lineages between the two disease entities and healthy controls, indicating that the pace of β-cell destruction is dictated by qualitative rather than numerical immune alterations. Transcriptome-derived pathway scores revealed diametrically opposed signalling landscapes: T1D displayed broad, pan-lineage activation of NF-κB, EGFR, MAPK and hypoxia programmes, whereas LADA was marked by a global suppression of NF-κB/EGFR cascades with selective retention of a moderate JAK–STAT tone. This molecular gradient establishes distinct inflammatory "set points" that are commensurate with the clinical velocity of autoimmunity.

Intercellular communication mapping further showed that LADA is enriched for inhibitory checkpoints, most notably HLA-C/F engagement of KIR2DL3/3DL1 on NK cells and reinforcement of the HLA-C–CD8A/B–LCK co-receptor complex, thereby raising the activation threshold of cytotoxic effectors while preserving low-affinity autoreactivity. In striking contrast, T1D is driven by an expansive TNF-centred crosstalk, augmented MHC-II trafficking and coordinated erosion of adhesion and homing signals, all of which synergistically potentiate systemic inflammation and tissue infiltration. Metabolically, basigin-mediated lactate export is preserved in LADA but suppressed in type 1 diabetes, suggesting greater glycolytic stress in the latter, while the CLEC2D–KLRB1 (LLT-1–CD161) axis is uniquely up-regulated in LADA, sustaining tissue-resident MAIT/γδ T-cell activity and low-grade inflammation.

The absence of public T- or B-cell clonotypes across cohorts underscores that disease trajectory is governed by the cytokine milieu and checkpoint balance rather than convergent receptor

usage. Taken together, our findings refine the conceptual framework of autoimmune diabetes, positioning LADA and T1D at opposite ends of a continuum defined by the degree of inflammatory amplification versus inhibitory restraint. These findings refine, but do not resolve, the debate on whether LADA constitutes a separate disease entity or a slower trajectory within autoimmune diabetes. Clinically, the NF-κB/EGFR–JAK–STAT gradient offers a tractable molecular signature for early risk stratification, while the HLA-C–KIR and HLA-C–CD8A/B–LCK axes emerge as attractive targets for precision immunomodulation aimed at preserving residual β-cell function.

A key limitation is that our analyses were confined to peripheral blood rather than pancreatic tissue, which may not fully reflect the local immune environment at the site of β-cell destruction.

Author contributions

IIG and MVS conceived the research concept. IIG, ESP, AAZ, and AAM developed the wet-lab methodology, carried out the experiments, and performed initial data analyses. VIC designed and executed the bioinformatic pipeline, validated the results, and, together with IIG and MDS, generated the figures. YVD, TVN, EVB, MYL, and YAM provided scientific expertise. DNL and RIK, NAS contributed to data interpretation. IRM, MVS and NGM acquired funding, provided project administration, and supervised the study. IIG and VIC wrote the first draft of the manuscript; all authors critically revised, edited, and approved the final version. The order of co–first authors was determined by the relative role in conception and design of the original study, with NGM and IID being the study initiator.

Acknowledgments

This research was funded by the Ministry of Science and Higher Education of the Russian Federation (agreement No. 075-15-2024-645 from 12 July 2024).

References

1. Hu J, et al. Latent Autoimmune Diabetes in Adults (LADA): From Immunopathogenesis to Immunotherapy. *Frontiers in Endocrinology*. 2022;13:917169.
2. Ravikumar V, et al. A Review on Latent Autoimmune Diabetes in Adults. *Cureus*. 2023;15(10):e47915.
3. Leslie RDG, et al. Diabetes classification: grey zones, sound and smoke: Action LADA 1. *Diabetes/Metabolism Research and Reviews*. 2008;24(7):511-519.
4. Tan T, et al. Variable frequencies of peripheral T-lymphocyte subsets in the diabetes spectrum from type 1 diabetes through latent autoimmune diabetes in adults (LADA) to type 2 diabetes. *Front Immunol*. 2022;13:974864.
5. Guo M, et al. A novel subpopulation of monocytes with a strong interferon signature indicated by SIGLEC-1 is present in patients with in recent-onset type 1 diabetes. *Diabetologia*. 2024;67(4):623-640.
6. Padmos RC, et al. Distinct monocyte gene-expression profiles in autoimmune diabetes. *Diabetes*. 2008;57(10):2768-73.
7. Xing Y, et al. Abnormal Neutrophil Transcriptional Signature May Predict Newly Diagnosed Latent Autoimmune Diabetes in Adults of South China. *Front Endocrinol (Lausanne)*. 2020;11:581902.
8. Ji Y, et al. Comparative Analysis of the Transcriptome of Latent Autoimmune Diabetes in Adult (LADA) Patients from Eastern China. *J Diabetes Res*. 2019;2019:8616373.
9. Rezaee A, et al. NF-κB axis in diabetic neuropathy, cardiomyopathy and nephropathy: A roadmap from molecular intervention to therapeutic strategies. *Heliyon*. 2024;10(9):e29871.
10. Sheng L, et al. Epidermal Growth Factor Receptor: A Potential Therapeutic Target for Diabetic Kidney Disease. *Front Pharmacol*. 2020;11:598910.
11. Russell MA, et al. The role of the interferon/JAK-STAT axis in driving islet HLA-I hyperexpression in type 1 diabetes. *Front Endocrinol (Lausanne)*. 2023;14:1270325.
12. Deng C, et al. Altered Peripheral B-Lymphocyte Subsets in Type 1 Diabetes and Latent Autoimmune Diabetes in Adults. *Diabetes Care*. 2015;39(3):434-440.

13. Wang Y, et al. High frequency of activated NKp46(+) natural killer cells in patients with new diagnosed of latent autoimmune diabetes in adults. *Autoimmunity*. 2015;48(4):267-73.
14. Hicks SC, et al. Missing data and technical variability in single-cell RNA-sequencing experiments. *Biostatistics*. 2017;19(4):562-578.
15. Zhao Y, et al. NF-κB in type 1 diabetes. *Inflamm Allergy Drug Targets*. 2011;10(3):208-17.
16. Sia C. Is a new immune response mediator in the NF-kappaB pathway--SUMO-4--related to type 1 diabetes? *Rev Diabet Stud*. 2005;2(2):58-60.
17. Liu T, et al. NF-κB signaling in inflammation. *Signal Transduct Target Ther*. 2017;2(17023-.
18. Shraim BA, et al. The Role of Epidermal Growth Factor Receptor Family of Receptor Tyrosine Kinases in Mediating Diabetes-Induced Cardiovascular Complications. *Frontiers in Pharmacology*. 2021;12:701390.
19. Song Z, et al. Epidermal Growth Factor Receptor Signaling Regulates β Cell Proliferation in Adult Mice. *J Biol Chem*. 2016;291(43):22630-22637.
20. Raugh A, et al. The amphiregulin/EGFR axis has limited contribution in controlling autoimmune diabetes. *Scientific Reports*. 2023;13(1):18653.
21. Zhou M, et al. JAK inhibitors: a new choice for diabetes mellitus? *Diabetology & Metabolic Syndrome*. 2025;17(1):33.
22. Waibel M, et al. Baricitinib and β-Cell Function in Patients with New-Onset Type 1 Diabetes. *New England Journal of Medicine*. 2023;389(23):2140-2150.
23. Trivedi PM, et al. Repurposed JAK1/JAK2 Inhibitor Reverses Established Autoimmune Insulitis in NOD Mice. *Diabetes*. 2017;66(6):1650-1660.
24. Nakayama M and AW Michels. Using the T Cell Receptor as a Biomarker in Type 1 Diabetes. *Front Immunol*. 2021;12:777788.
25. Japp AS, et al. TCR(+)/BCR(+) dual-expressing cells and their associated public BCR clonotype are not enriched in type 1 diabetes. *Cell*. 2021;184(3):827-839.e14.
26. Linsley PS, et al. Germline-like TCR-α chains shared between autoreactive T cells in blood and pancreas. *Nature Communications*. 2024;15(1):4971.
27. Seay HR, et al. Tissue distribution and clonal diversity of the T and B cell repertoire in type 1 diabetes. *JCI Insight*. 2016;1(20):e88242.

28. Ahmed R, et al. A Public BCR Present in a Unique Dual-Receptor-Expressing Lymphocyte from Type 1 Diabetes Patients Encodes a Potent T Cell Autoantigen. *Cell*. 2019;177(6):1583-1599.e16.

29. Boehm BO and JA Bluestone. Differential roles of costimulatory signaling pathways in type 1 diabetes mellitus. *Rev Diabet Stud*. 2004;1(4):156-64.

30. Pohlkamp T, et al. Functional Roles of the Interaction of APP and Lipoprotein Receptors. *Frontiers in Molecular Neuroscience*. 2017;1:54.

31. UniProt. Alpha-2-macroglobulin receptor-associated protein (UniProtKB P30533). https://www.uniprot.org/uniprotkb/P30533/entry. Updated 2025. Accessed June 10, 2025.

32. Srinivasan S, et al. Structure, function, and immunomodulation of the CD8 co-receptor. *Frontiers in Immunology*. 2024;15:1412513.

33. Moradi S, et al. Structural plasticity of KIR2DL2 and KIR2DL3 enables altered docking geometries atop HLA-C. *Nature Communications*. 2021;12(1):2173.

34. Raulet DH. Missing self recognition and self tolerance of natural killer (NK) cells. *Seminars in Immunology*. 2006;18(3):145-150.

35. Soltani S, et al. Association of KIR gene polymorphisms with Type 1 Diabetes: a meta-analysis. *J Diabetes Metab Disord*. 2020;19(2):1777-1786.

36. Agnello L, et al. The Role of Killer Ig-like Receptors in Diseases from A to Z. *Int J Mol Sci*. 2025;26(7):3242.

37. Long L, et al. The promising immune checkpoint LAG3: from tumor microenvironment to cancer immunotherapy. *Genes Cancer*. 2018;9(5-6):176-189.

38. Cruikshank WW, et al. Interleukin-16. *J Leukoc Biol*. 2000;67(6):757-66.

39. Zhao Y, et al. Toxins Targeting the Kv1.3 Channel: Potential Immunomodulators for Autoimmune Diseases. *Toxins (Basel)*. 2015;7(5):1749-64.

40. Pober JS and WC Sessa. Evolving functions of endothelial cells in inflammation. *Nature Reviews Immunology*. 2007;7(10):803-815.

41. Łacina P, et al. BSG and MCT1 Genetic Variants Influence Survival in Multiple Myeloma Patients. *Genes (Basel)*. 2018;9(5):226.

42. Peralta RM, et al. Dysfunction of exhausted T cells is enforced by MCT11-mediated lactate metabolism. *Nature Immunology*. 2024;25(12):2297-2307.

43. Zirlik A, et al. CD40 Ligand Mediates Inflammation Independently of CD40 by Interaction With Mac-1. *Circulation*. 2007;115(12):1571-1580.

44. Konduri V, et al. CD8+CD161+ T-Cells: Cytotoxic Memory Cells With High Therapeutic Potential. *Frontiers in Immunology*. 2021;11:613204.

45. Lu J, et al. Cytokines in type 1 diabetes: mechanisms of action and immunotherapeutic targets. *Clin Transl Immunology*. 2020;9(3):e1122.

46. Litonjua AA, et al. Very important pharmacogene summary ADRB2. *Pharmacogenet Genomics*. 2010;20(1):64-9.

47. GeneCards. KCNQ5 Gene – GeneCards. https://www.genecards.org/cgi-bin/carddisp.pl?gene=KCNQ5. Updated 2025. Accessed May 10, 2025.

48. Zhu X and J Zhu. CD4 T Helper Cell Subsets and Related Human Immunological Disorders. *Int J Mol Sci*. 2020;21(21):8011.

49. Obasanmi G, et al. Peripheral Blood Mononuclear Cells from Patients with Type 1 Diabetes and Diabetic Retinopathy Produce Higher Levels of IL-17A, IL-10 and IL-6 and Lower Levels of IFN-γ-A Pilot Study. *Cells*. 2023;12(3):467.

50. Aghili B, et al. Altered Suppressor Function of Regulatory T Cells in Type 1 Diabetes. *Iran J Immunol*. 2015;12(4):240-51.

51. Hull CM, et al. Regulatory T cell dysfunction in type 1 diabetes: what's broken and how can we fix it? *Diabetologia*. 2017;60(10):1839-1850.

52. Hampe CS. B Cell in Autoimmune Diseases. *Scientifica (Cairo)*. 2012;2012:215308.

53. Guzzo C, et al. Interleukin-27 induces a STAT1/3- and NF-kappaB-dependent proinflammatory cytokine profile in human monocytes. *J Biol Chem*. 2010;285(32):24404-11.

54. Li Y, et al. Revisiting the Antigen-Presenting Function of β Cells in T1D Pathogenesis. *Frontiers in Immunology*. 2021;12:690783.

55. Jacobsen LM, et al. T Cell Receptor Profiling in Type 1 Diabetes. *Current Diabetes Reports*. 2017;17(11):118.

56. Qin H, et al. Natural killer cells from children with type 1 diabetes have defects in NKG2D-dependent function and signaling. *Diabetes*. 2011;60(3):857-66.

57. Trivedi P, et al. Perforin facilitates beta cell killing and regulates autoreactive CD8+ T-cell responses to antigen in mouse models of type 1 diabetes. *Immunol Cell Biol*. 2016;94(4):334-41.

58. Sharma RB, et al. Living Dangerously: Protective and Harmful ER Stress Responses in Pancreatic β-Cells. *Diabetes*. 2021;70(11):2431-2443.

59. Roy S, et al. Decoding the Immune Dance: Unraveling the Interplay Between Beta Cells and Type 1 Diabetes. *Molecular Metabolism*. 2024;88:101998.

60. Shimada A, et al. The role of the CXCL10/CXCR3 system in type 1 diabetes. *Rev Diabet Stud*. 2009;6(2):81-4.

61. Ahlmann-Eltze C and W Huber. Comparison of transformations for single-cell RNA-seq data. *Nature Methods*. 2023;20(5):665-672.

62. Badia-i-Mompel Pa. decoupleR: ensemble of computational methods to infer biological activities from omics data. *Bioinformatics Advances*. 2022;2(1):vbac016.

63. Butler A, et al. Azimuth: A shiny app demonstrating a query-reference mapping algorithm for single-cell data. https://satijalab.github.io/azimuth/index.html. Updated 2021. Accessed June 11, 2025.

64. Chechekhina E, et al. scParadise: Tunable highly accurate multi-task cell type annotation and surface protein abundance prediction. *bioRxiv*. 2024;

65. Gayoso A, et al. A Python library for probabilistic analysis of single-cell omics data. *Nature biotechnology*. 2022;40(2):163-166.

66. Hao Y, et al. Dictionary learning for integrative, multimodal and scalable single-cell analysis. *Nature biotechnology*. 2024;42(2):293-304.

67. Heumos L, et al. Pertpy: an end-to-end framework for perturbation analysis. *bioRxiv*. 2024;2008--2024.

68. Kolberg L, et al. g: Profiler—interoperable web service for functional enrichment analysis and gene identifier mapping (2023 update). *Nucleic acids research*. 2023;51(W1):W207----W212.

69. Korsunsky I, et al. Fast, sensitive and accurate integration of single-cell data with Harmony. *Nature methods*. 2019;16(12):1289--1296.

70. Lotfollahi M, et al. scGen predicts single-cell perturbation responses. *Nature methods*. 2019;16(8):715-721.

71. Luecken MD, et al. Benchmarking atlas-level data integration in single-cell genomics. *Nature methods*. 2022;19(1):41-50.

72. Muzellec B, et al. PyDESeq2: a python package for bulk RNA-seq differential expression analysis. *Bioinformatics*. 2023;39(9):btad547.

73. Polaski K, et al. BBKNN: fast batch alignment of single cell transcriptomes. *Bioinformatics*. 2020;36(3):964--965.

74. Stuart T, et al. Comprehensive integration of single-cell data. *Cell*. 2019;177(7):1888--1902.

75. Wolf FA, et al. SCANPY: large-scale single-cell gene expression data analysis. *Genome biology*. 2018;19(1-5.

76. Xi NM and JJ Li, *Benchmarking computational doublet-detection methods for single-Cell RNA sequencing data*. 2021. p. 176-194.

77. Young MD and S Behjati. SoupX removes ambient RNA contamination from droplet-based single-cell RNA sequencing data. *Gigascience*. 2020;9(12):giaa151.

78. Dimitrov D, et al. LIANA+ provides an all-in-one framework for cell–cell communication inference. *Nature Cell Biology*. 2024;26(9):1613-1622.

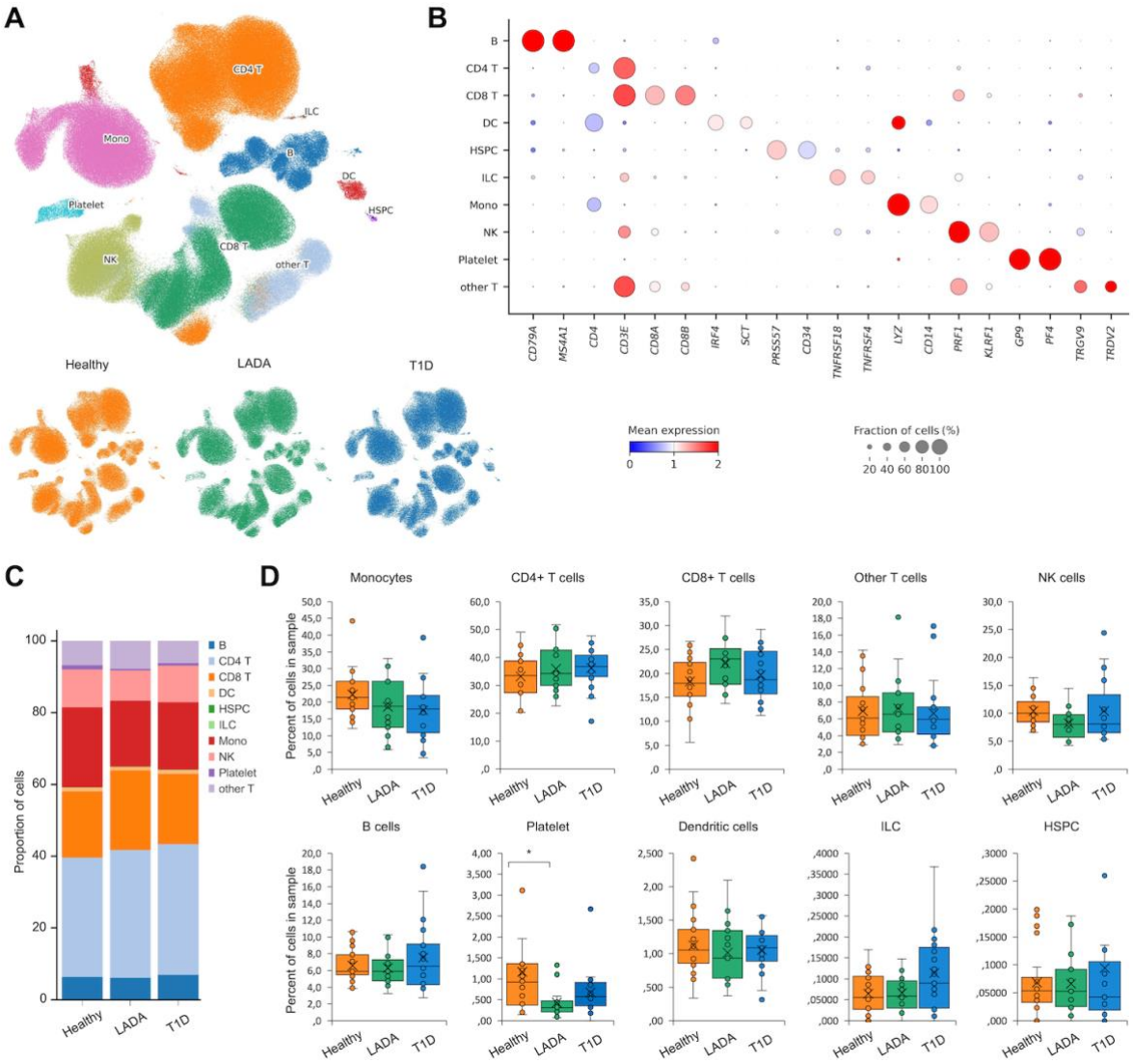

Figure 1. Atlas of PBMC from healthy donors and patients with latent autoimmune diabetes mellitus (LADA) and type 1 diabetes (T1D). (**A**) Uniform manifold approximation and projection (UMAP) of transcriptional profiles of PBMC (n = 442655 cells). Each cell type cluster was shown in a different color. Healthy, healthy individuals; LADA, patients with latent autoimmune diabetes mellitus; T1D, patients with type 1 diabetes. (**B**) Average expression of known marker genes in indicated cell types. The dot size represents percent of cells expressing the genes in each cell type. The expression intensity of markers is shown. (**C**) Proportion of major cell types shown in bar plots in different donor states (Healthy, LADA, T1D). (**D**) Compositional analysis of major cell types in healthy individuals and patients with latent autoimmune diabetes mellitus (LADA) and type 1 diabetes (T1D). One-way ANOVA with post-hoc Dunn test. Median (line), mean (cross), n = 15-22 (dots), *p < 0.05.

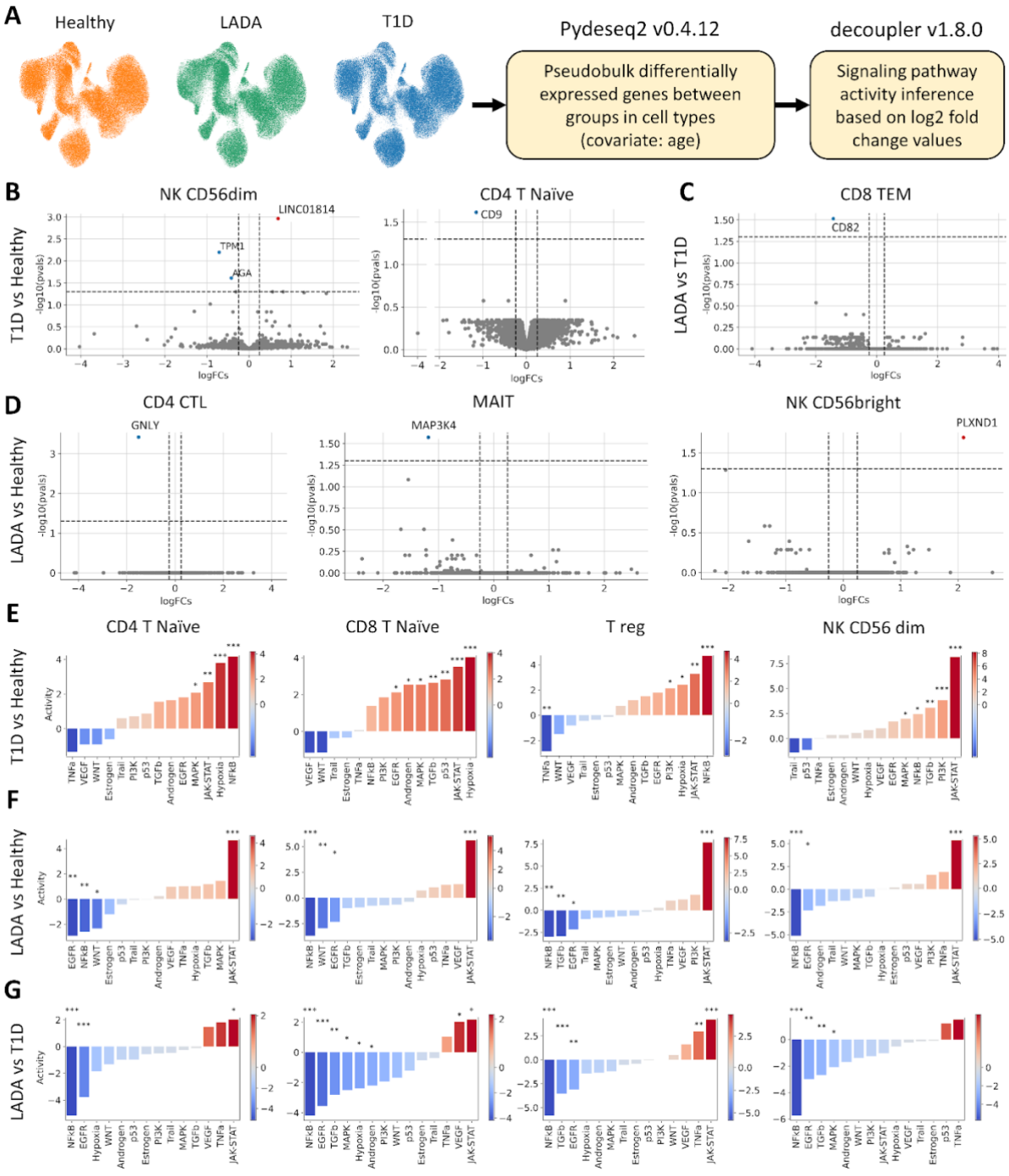

Figure 2. Signaling pathway activity inference in immune cells of healthy donors and patients with latent autoimmune diabetes mellitus (LADA) and type 1 diabetes (T1D). (**A**) Scheme of differential gene expression analysis and pathway activity inference. (**B-D**) Volcano plots of differentially expressed genes in cell subtypes between patients with type 1 diabetes (T1D) and healthy donors (**B**), patients with latent autoimmune diabetes mellitus (LADA) and patients with type 1 diabetes (**C**), patients with latent autoimmune diabetes mellitus (LADA) and healthy donors (**D**). Wald test with Benjamini-Hochberg p-value correction. Thresholds in plots: log2 fold change > 0.25, p adjusted < 0.05. (**E-G**) Bar plots of differentially activated signaling pathways in cell between patients with type 1 diabetes (T1D) and healthy donors (**E**), patients with latent autoimmune diabetes mellitus (LADA) and healthy donors (**F**), patients with latent autoimmune diabetes mellitus (LADA) and patients with type 1 diabetes (**G**). Student's t-test with Benjamini-Hochberg p-value correction. *p < 0.05, ** p < 0.01, *** p < 0.001.

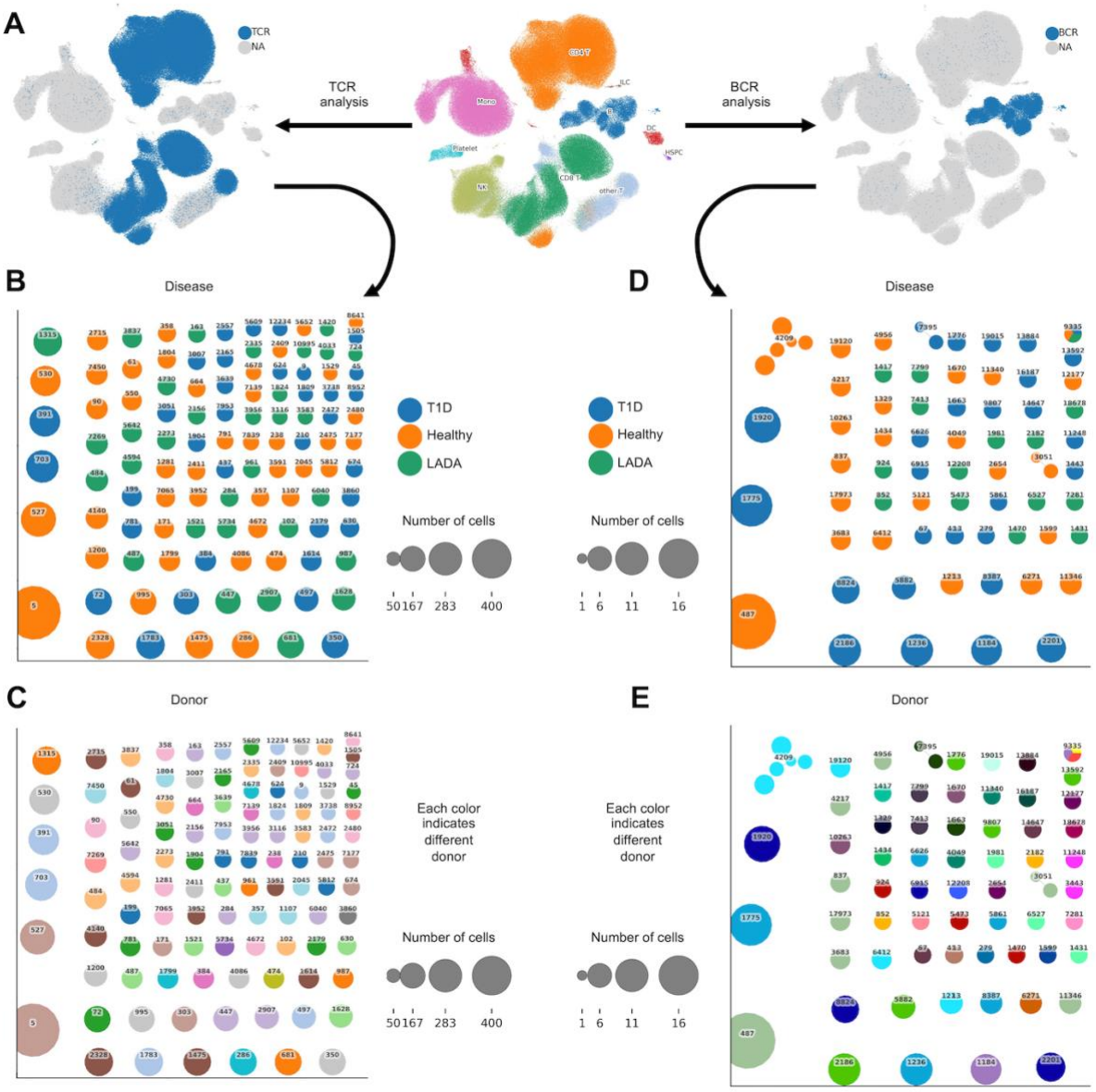

Figure 3. Immune receptor profiling of T and B cells of healthy donors and patients with latent autoimmune diabetes mellitus (LADA) and type 1 diabetes (T1D). (**A**) Quality control of T cell receptor and B cell receptor data. (**B**) Disease-specific T cell receptor clonotype network. Each dot represents a different clone. Each color indicates a different condition: healthy donors (orange), patients with latent autoimmune diabetes mellitus (LADA, green), and type 1 diabetes (T1D, blue). (**C**) Donor-specific T cell receptor clonotype network. Each dot represents a different clone. Each color indicates a different donor. (**D**) Disease-specific B cell receptor clonotype network. Each dot represents a different clone. Each color indicates a different condition: healthy donors (orange), patients with latent autoimmune diabetes mellitus (LADA, green), and type 1 diabetes (T1D, blue). (**E**) Donor-specific B cell receptor clonotype network. Each dot represents a different clone. Each color indicates a different donor. Grouped clones share at least 80% sequence similarity.

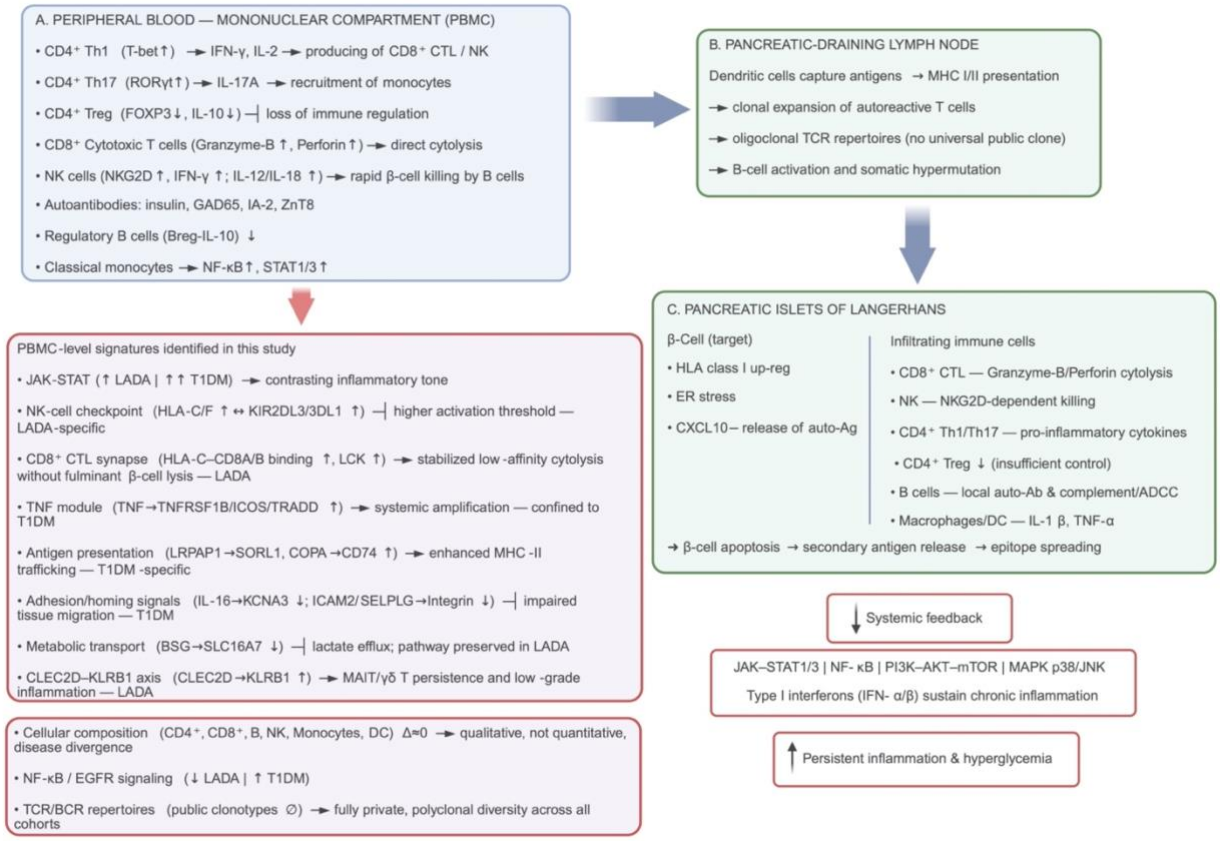

Figure. 4. Model of T1D and LADA pathogenesis based on published literature and our own findings. Panel A illustrates the peripheral-blood mononuclear-cell (PBMC) compartment, where heightened activity of $CD4^+$ Th1/Th17, $CD8^+$ cytotoxic T lymphocytes (CTLs) and natural-killer (NK) cells, coupled with depletion of $FOXP3^+$ regulatory T cells (Tregs) and IL-10-producing B-regulatory cells (Bregs), establishes a pro-inflammatory milieu and systemic production of disease-defining autoantibodies. **Panel B** depicts the pancreatic-draining lymph node: dendritic cells (DCs) ferry β-cell antigens, driving oligoclonal expansion of autoreactive T-cell receptors (TCRs) without a universal public clonotype. **Panel C** illustrates the islet microenvironment, where upregulation of HLA class I molecules and endoplasmic reticulum stress in β-cells result in their direct lysis by $CD8^+$ cytotoxic T lymphocytes (CTLs) and natural killer (NK) cells. In addition, β-cells are subject to cytokine-mediated damage driven by Th1 and Th17 cells, antibody-dependent cellular cytotoxicity (ADCC), and the effects of innate cytokines released by macrophages and dendritic cells. **The bottom left panel** displays data generated in the present study. Integrated JAK–STAT1/3, NF-κB, PI3K–AKT–mTOR, MAPK p38/JNK pathways maintain chronic inflammation and propagate β-cell apoptosis, leading to epitope spreading and progressive loss of insulin secretion. Created in BioRender. Samsonova, M. (2025) https://BioRender.com/tkecn1v

Table 1. Functional consolidation of differentially regulated ligand–receptor axes in the PBMC of T1D versus Healthy Controls

Functional module	Ligand-receptor pairs (↑/↓)	Predominant source subsets	Principal recipient clusters	Pathobiological interpretation
1. TNF-centred inflammatory & co-stimulatory circuitry	TNF→VSIR ↑ TNF→TNFRSF1B ↑ TNF→ICOS ↑ TNF→TRADD ↑	CD4 TCM, CD8 TEM; minor input from Treg	Broad CD4 and CD8 memory/effector pool, MAIT, NK, γδ T	Amplified TNF signaling engages canonical pro-inflammatory pathways via TNFRSF1B and TRADD, while concurrently promoting an inflammatory environment that facilitates co-stimulatory (ICOS) and immunomodulatory (VSIR) activity. This may collectively lower activation thresholds and promote the persistence of effector and memory phenotypes.
2. Antigen-processing & MHC-II trafficking	LRPAP1→SORL1 ↑ COPA→CD74 ↑	Naïve and memory CD4/CD8 T cells, Treg	Virtually all T-cell subsets	Up-regulation of endocytic chaperones (SORL1) and trafficking regulator (CD74) suggests increased peptide loading dynamics, potentially enlarging the β-cell-derived autoantigenic repertoire

				recognised by autoreactive T cells.
3. Cytoskeletal phosphatase tuning of TCR signalling	SPTAN1→PTPRA ↑	Global CD4/CD8, Treg	All subsets	Interaction between spectrin α-chain (SPTAN1) and the Src-family phosphatase PTPRA may contribute to the remodeling of membrane microdomains, thereby lowering the activation threshold of the T cell receptor (TCR) and facilitating aberrant clonal expansion.
4. Adhesion & tissue-trafficking checkpoint (globally attenuated)	IL16→KCNA3 ↓ ICAM2→ITGAM_ITGB2 ↓ ICAM2→ITGAL_ITGB2 ↓ SELPLG→ITGB2 ↓ SELPLG→SELL ↓ CLEC11A→ITGB1↓	naïve and central/memory $CD4^+$/$CD8^+$ T cells	TRM (CD103/CD49a), CTL, MAIT, NK, γδ T	A coordinated reduction in adhesion molecule interactions, including selectin-, integrin-, and IL-16–KCNA3-mediated pathways, suggests impaired transendothelial migration and reduced tissue residency. This phenotype may reflect functional exhaustion or defective peripheral homing within the effector

				and memory compartments.
5. Metabolic balance & lactate shuttling	BSG (basigin)→SLC16A7 ↓	naïve and memory $CD4^+$/$CD8^+$ T cells, Tregs	Wide T-cell spectrum, incl. NK	Downregulation of the basigin–SLC16A7 axis suggests impaired lactate export and reduced glycolytic flexibility, hallmarks of chronically stimulated lymphocytes in autoimmune contexts. This metabolic constraint may contribute to dysfunctional immune persistence and effector fatigue.
6. NK-cell inhibitory checkpoint erosion	B2M→KLRC1 ↓ B2M→KLRD1↓	naïve and memory $CD4^+$/$CD8^+$ T cells, Tregs	NK CD56dim/bright, γδ T, TRM	Attenuated delivery of β2-microglobulin to KLRC1/CD94 receptors compromises inhibitory signaling in cytotoxic lymphocytes. This erosion of checkpoint control may predispose NK and γδ T cells to enhanced cytolytic activity against pancreatic β-cells in type 1 diabetes.

7. Alternative CD40L signalling arm	CD40LG→ITGAM_ITGB2 ↓ CD40LG→CD53↓	Naïve and memory CD4 pools	Broad myeloid-interacting subsets	Downregulation of CD40L interactions with integrin ITGAM/ITGB2 and the tetraspanin CD53 may disrupt non-canonical T cell–APC contact sites, independent of classical CD40 signaling. This could attenuate reciprocal activation loops and dampen downstream inflammatory amplification in the autoimmune milieu.

Table 2. Functional consolidation of differentially regulated ligand–receptor axes in the PBMC of LADA versus Healthy Controls

Functional module	Ligand-receptor pairs (↑/↓)	Predominant source subsets	Principal recipient clusters	Pathobiological interpretation
1. MHC-I–KIR checkpoint calibration	HLA-F → KIR3DL1↑ HLA-C → KIR2DL3↑ HLA-C → KIR3DL1↑	CD4 T naïve, TCM, TEM; CD8 T naïve, TCM, TEM; Treg	NK CD56dim	Upregulation of classical and non-classical MHC-I ligands (HLA-C, HLA-F) on T cells enhances inhibitory signaling through KIR2DL3 and KIR3DL1 on NK cells. This may promote NK-cell "education" and raise the activation threshold, thereby limiting non-specific β-cell cytotoxicity, a mechanism consistent with the indolent autoimmune trajectory of LADA.
2. MHC-I–CD8 co-receptor reinforcement	HLA-F → CD8B↑ HLA-C → CD8A↑ HLA-C → CD8B↑	Same as module 1	CD8 TRM (CD103/CD49a), CD8 T naïve, TCM, TEM, MAIT	Enhanced presentation of classical and non-classical MHC-I molecules (HLA-C, HLA-F) promotes stronger engagement of CD8 co-receptors, stabilizing the TCR–pMHC interface. This may lower the activation threshold of autoreactive cytotoxic T cells, fostering a persistent but non-fulminant effector state characteristic of the indolent progression in LADA.

3. MHC-II–driven antigen presentation & LAG3 checkpoint	HLA-DPB1 → CD4↑ HLA-DPB1 → LAG3↑ HLA-DRB5 → LAG3↑	CD4 TCM, TEM; CD8 T naïve, TCM, TEM; Treg	CD4 CTL, CD4 T naïve, TCM, TEM, TRM; MAIT; γδ T	Increased expression of MHC-II molecules (HLA-DPB1, HLA-DRB5) on T cells enhances both CD4 co-receptor engagement and LAG3–mediated inhibitory signaling. This dual signaling axis suggests a dynamic tension between antigen-driven activation and negative feedback regulation, potentially balancing autoaggressive and self-tolerant programs within the $CD4^+$ T cell compartment in LADA.
4. CLEC2D–KLRB1 innate-like T/NK modulation	CLEC2D → KLRB1↑	Broad naïve & memory CD4/CD8 pools, Treg	TRM, CTL, CD4/8 TEM, MAIT, NK $CD56^{bright/dim}$, γδ T	Increased interaction between CLEC2D and the KLRB1 receptor supports the persistence and effector function of MAIT and γδ T cells. This signaling axis promotes IL-17 and IFN-γ production and may sustain low-grade, tissue-resident inflammation, a hallmark of the indolent autoimmune profile observed in LADA.

5. Complement & adhesion checkpoint attenuation	CD55 → ADGRE5↓ VIM → CD44 ↓	All CD4 & CD8 states, Treg	broad lymphoid and innate-like populations	Downregulation of the CD55–ADGRE5 and vimentin (VIM) – CD44 axes may compromise both complement regulation and cell–matrix adhesion. This attenuation could restrict effector cell extravasation but may also impair tissue repair and resolution of inflammation, aligning with the persistent, low-grade immunopathology characteristic of LADA.

Table 3. Functional consolidation of differentially regulated ligand–receptor axes in the PBMC of LADA versus T1D

Functional module	**Ligand-receptor pairs (↑/↓)**	**Predominant source subsets***	**Principal recipient clusters***	**Pathobiological interpretation**
1. NK-cell inhibitory checkpoint intensification	HLA-C → KIR2DL3↑ HLA-C → KIR3DL1↑	CD4/8 T naïve, TCM, TEM; Treg	NK CD56bright	Upregulated expression of classical MHC-I ligands (HLA-C) on T cells enhances inhibitory signaling through KIR2DL3 and KIR3DL1 on CD56bright NK cells. This likely elevates their activation threshold, curbing non-specific cytolytic activity. The resulting tempering of innate immune pressure on β-cells aligns with the slower and more indolent β-cell attrition observed in LADA relative to T1D

2. CD8:TCR avidity reinforcement	HLA-C → CD8A↑; HLA-C → CD8B↑; LCK → CD8A/B heterodimer↑	Same as module 1	CD8 TRM (CD103/CD49a), CD8 naïve, TCM, TEM, MAIT	Enhanced engagement of MHC-I (HLA-C) with CD8 co-receptors, coupled with increased association of LCK kinase with the CD8A/B heterodimer, reinforces the pMHC–TCR complex. This configuration lowers the activation threshold of autoreactive cytotoxic T cells, promoting a persistent, low-intensity effector response rather than the abrupt cytolytic surge typical of fulminant T1D.
3. TNF-superfamily crosstalk to regulatory NK cells	LTB → TNFRSF1A↑	Same as module 1	NK CD56bright	Upregulated lymphotoxin-β (LTB) signaling via TNFR1 (TNFRSF1A) in CD56bright NK cells may enhance IFN-γ–driven regulatory functions without triggering the full pro-inflammatory cascade typically associated with TNFA in T1D. This

				restrained activation profile may contribute to moderated inflammation and slower β-cell loss in LADA.
4. Innate-like T/NK maintenance via LLT-1–CD161	CLEC2D → KLRB1↑	Broad naïve & memory CD4/8 pools; Treg	TRM, CTL, TEM, MAIT, NK $CD56^{bright/dim}$, γδ T	Increased LLT-1 (CLEC2D) signaling through the CD161 receptor (KLRB1) supports the maintenance and effector functions of MAIT and γδ T cells. This promotes tissue-resident inflammation driven by IL-17 and IFN-γ production, yet circumvents the overt Th1 polarization and fulminant cytotoxicity characteristic of T1D.

5. Adrenergic/ion-channel neuro-immune tuning	ARPC5 → ADRB2↑; CALM3 → KCNQ5↑	Same as module 1	ADRB2- or KCNQ5-positive CD4/8 TEM, MAIT, NK	Upregulated neuro-immune signaling via β_2-adrenergic receptors (ADRB2) and Ca^{2+}/K^{+} channel modulation (CALM3–KCNQ5) suggests enhanced sympathetic and ionic control over effector lymphocytes. This may contribute to stress-responsive fine-tuning of inflammation, aligning with the controlled and indolent autoimmune progression characteristic of LADA.
6. Complement-adhesion checkpoint erosion	CD55 → ADGRE5↓	All CD4/8 states; Treg	Nearly all lymphoid & innate-like subsets	Downregulation of the CD55–CD97 axis diminishes complement regulation and weakens cell–matrix adhesion. This may restrict aggressive tissue infiltration, typical of fulminant T1D, but also impairs inflammation resolution, contributing to the low-grade, chronic

				immune activity characteristic of LADA.

Table 4. Eligibility Criteria for Study Participants

Group	Inclusion Criteria	Exclusion Criteria
All Participants	- Age 18–55 years - Male or female - BMI ≤35 kg/m² - Signed informed consent	- Presence of other systemic autoimmune diseases - History of pancreatic disorders or prior pancreatic surgery - Use of immunosuppressive therapy within the past 12 months - Receipt of any vaccination within 3 months prior to enrollment - History of respiratory viral infection within 3 months prior to enrollment - Current pregnancy
T1D Group	- Confirmed diagnosis of type 1 diabetes mellitus - Disease duration ≤1 year	Same as above
LADA Group	- Positive β-cell autoantibodies (anti-GAD >10 U/mL, ICA >1 U/mL, anti-insulin >10 U/mL, or anti-IA2 >10 U/mL) - No insulin requirement for ≥6 months post-diagnosis	Same as above

Healthy Controls	- No history of diabetes, impaired fasting glucose, or impaired glucose tolerance - Meets general inclusion criteria	Same as above

Supplementary

Supplementary Table S1. Baseline clinical characteristics of study participants

Parameter	**T1D (*n* = 21)**	**LADA (*n* = 15)**	**Healthy Controls (*n* = 22)**	***P*-value**
Male sex, *n* (%)	10 (48%)	7 (47%)	11 (50%)	> 0.05
Age, years	26 [21; 31]	40 [34; 45]	33.5 [27; 42]	< 0.001
Disease duration, months	6 [2; 8]	38 [19; 53]	Not applicable	< 0.001
BMI, kg/m²	22.3 [20.1; 23.8]	23.0 [20.1; 23.9]	24.8 [20.6; 28.3]	0.214
HbA1c, %	7.8 [6.4; 10.4]	7.1 [6.6; 8.8]	5.1 [4.9; 5.4]	< 0.001

Legend: Statistical comparisons were performed using the chi-square test for categorical variables (male sex), Kruskal–Wallis test for continuous variables across all groups, and Mann–Whitney U test for pairwise comparison of disease duration between T1D and LADA.

Abbreviations: T1D, type 1 diabetes; LADA, latent autoimmune diabetes in adults; BMI, body mass index; HbA1c, glycated hemoglobin.